Copper electrodeposition in a deep eutectic solvent. First stages analysis considering Cu(I) stabilization in chloride media

P. Sebastián, E. Vallés, E. Gómez*,

Departament de Química Física and Institut de Nanociència i Nanotecnologia (IN^{2}UB), Universitat de Barcelona, Martí i Franquès 1, E-08028 Barcelona, Spain.

*Author to whom correspondence should be addressed

e-mail: e.gomez@ub.edu

Phone: 34 934 021 234

Fax: 34 934 021 231

Abstract

The aim of the present work is to study copper electrocrystallization in a Deep Eutectic Solvent (DES) (eutectic mixture of choline chloride and urea 1:2) as electrolyte, paying special attention to the influence of the liquid on the nucleation mechanism. Deposition process was studied from both Cu(II) and Cu(I) solutions. As the DES solvent is chloride rich, a parallel analysis was made in aqueous solution containing an excess of chloride to compare medium influence on nucleation mechanism. While copper (I) can be directly electrodeposited from chloride excess solutions, copper (II) electrodeposition takes place via a separate step in which Cu(II) is firstly reduced to Cu(I). A methodology is proposed for studying mechanistic aspects of the early stages of copper electrodeposition from the Cu(II) chloride solutions. For all solutions, cyclic voltammetry was used to establish the potential range at which copper electrodeposition occurred, while potentiostatic technique was used to study the nucleation mechanism. In all media, deposition follows a nucleation and three-dimensional growth controlled by diffusion. The diffusion coefficient of Cu(I) species present in the solution has been calculated from potentiostatic curves by logarithmic linear regression of j vs $t^{-1/2}$ at long deposition times, whereas the same parameter for copper (II) was calculated from cyclic voltammetry, taking advantage from the process quasi -reversibility. The viability of the nucleation mechanism by Scharifker-Hills model was demonstrated by the analysis of the rising part of the j-t transients independently of the selected solution.

Keywords: copper electrodeposition, first stages, DES solvent, chloride effect

1. Introduction

Copper electrodeposition plays a key role in electronics, particularly in printed circuit manufacture and especially for circuit interconnections in which copper has progressively replaced aluminium [1]. However, while copper deposits have been widely used to form thin and thick coatings, relatively few experiments have been conducted to study the first deposition stages and the role of the solution chemical nature on the deposition process [2-7]. It is well known that the characteristics of final deposits depend primarily on the plating solution composition. In particular, the presence of free or complex cations is an important factor, because they do strongly affect both nucleation and growth.

In the last decade, ionic liquids have been used as alternative solvents in the plating solutions due to their low vapor pressure and because in most cases they are a less environmentally hazardous option [8]. Recently, a novel class of liquids named *Deep eutectic solvents* (DES) based on mixtures of choline chloride and hydrogen bond donors has been developed. These liquids are able to solubilize many different metal salts or metal oxides, so that they are being an alternative solvent for electrodeposition processes [9-12]. The DES show air and moisture stability, can be handled easily under environmental conditions, and the fact that they offer the first economically viable liquids that can be used in industrial scale makes them promising candidates when aqueous medium is not suitable [13].

The copper electrodeposition has been widely investigated by some authors both in aqueous and in ionic liquids, although most of the work was devoted to the preparation of coatings, but few gave reliable information of the first stages of the process [14-18]. Recently Abbot and coworkers [5] demonstrated that the use of ionic liquids based on eutectic mixtures of choline chloride and hydrogen bond donors such as urea or ethylene glycol can be used as convenient electrochemical solvents, in which copper reduction occurs via two well-separated one-electron stages: Cu(II)-Cu(I)-Cu. In these conditions of intermediate stabilization by the medium, the mechanistic analysis of the early stages of deposition process, by means the typical single potentiostatic step, does not lead to convincing results. The simultaneous contribution to the total current of the two reduction processes disturbs the quantitative analysis leading to unreliable interpretations.

Aiming to deepen the study of the early stages of copper electroplating process, this work is concerned with the copper deposit nucleation in conditions in which the intermediate Cu(I) is stabilized, in this case due to the presence of excess chloride in solution. Copper electrodeposition mechanism has been studied in two chemical systems that differ substantially due to the solvent used, a choline chloride-based deep eutectic solvent and an aqueous concentrated chloride solution, but having in common the presence of excess chloride, placing especial interest on the first stages of the copper electrocrystallization both from Cu(I) and Cu(II). The selected solvents present the necessary qualities to obtain an interesting comparison.

Both Cu(I) and Cu(II) solutions were used in order to study the copper deposition process in the selected solvents. When deposition from Cu(II) solutions was analyzed, taking into account the stabilization of intermediate Cu(I) in the chloride media, an innovative double potentiostatic step was proposed, in order to separate, as far as possible, currents related to the reduction of each copper species. The purpose of the Cu deposition study from the Cu(I) solution is to analyze the copper reduction stage leading directly to deposit. In all media, chloride high concentration allows Cu(I) solubilisation. In order to minimize deposition rate an amorphous substrate (vitreous carbon) has been selected and low ionic copper concentrations were analyzed. This substrate has the advantage of presenting poor interaction with metallic deposits and the low ionic copper concentration enables discriminating the currents related to first stages although it does complicate obtaining reproducible results. Previous voltammetric analysis allows defining the potential range at which processes take place in the different media whereas potentiostatic experiments results will provide the necessary data for the quantitative mechanistic analysis.

2. Experimental

Chemicals used were CuCl from Aesar, high purity, $CuCl_2$ $2H_2O$ and NaCl both from Merck, all of them of analytical grade. Aqueous solutions were prepared with water doubly distilled and then treated with a Millipore Milli-Q system and the pH was kept at 3. The DES solvent was prepared using choline chloride (from Across Organics) and urea (from Merck) of analytical grade; the solids, in the molar proportion 1 choline chloride: 2 urea, were warmed and removed constantly to achieve the liquid state. In the solution prepared with DES no support electrolyte was added taking advantage that DES acts both as solvent and as support electrolyte. After preparation, these solutions were placed in a desiccator in order to avoid uptake of water by higroscopicity.

A cylindrical thermostatized three electrode cell of one single compartment was used. Electrochemical experiments were carried out using an Autolab with PGSTAT30 equipment and GPES software. Basic electrochemical study was made using vitreous carbon (from Metrohm) as working electrode, oxidized until the current response lower than 10^{-7} A was recorded and then polished to a mirror finish using alumina of different grades (3.75 and 1.87 μm), cleaned ultrasonically for 2 min in water and immersed in the solution. The contact with the solution was by meniscus. The counter electrode was a spiral of platinum. The reference electrode was an Ag|AgCl/KCl 3M mounted in a Luggin capillary containing, upon depending the solvent, either NaCl 3M in aqueous solutions or the DES solvent when it was worked in the analogue ionic liquid medium. Stable and reproducible potential values were obtained with these reference electrodes [19].

Voltammetric experiments were carried out at 50 mV s^{-1}, scanning at first to negative potentials. Chronoamperometric experiments were performed starting from a potential where no process took place. All electrochemical experiments were made using freshly polished substrata. In aqueous media the working temperature was 30ºC, whereas the temperature selected in DES solvent was 70ºC to favour low viscosity and high conductivity of the solvent. Morphology was observed using a scanning electron microscope JEOL model JSM-6510 and a field emission scanning electron microscope JEOL JSM-7100F.

3. Results and discussion

3.1. Copper electrodeposition in DES. General behavior

In order to establish the potential range at which copper electrodeposition takes place in DES, cyclic voltammetry from a solution containing 0.05M $CuCl_2$ was recorded (Fig. 1 solid line). The voltammograms showed two groups of features sufficiently separated: firstly, the couple whose profile fits with that corresponding to a quasi-reversible reduction/oxidation process (C_1, A_1), and a second group (C_2, A_2) that appears at more negative potentials. The C_2 reduction peak shows a slow current increase leading to a wide peak prior to the current decay. Reversing the scan at the beginning of C_2 peak, the typical loop associated to a nucleation and growth mechanism was recorded (Fig. 1 dashed line), evidencing that the second group of features (C_2, A_2) corresponds to copper electrodeposition, the A_2 peak being related to copper deposit oxidation. Similar behavior was observed previously [5], in two well separated steps in which firtly a single electron is transferred, a fact that can be explained by considering copper (I) stabilization by complexation with chloride. The fact that the overall deposition process takes place via two widely separated processes encouraged us to analyze each one separately. At first it was decided to analyze the stage of copper electrodeposition using a solution containing 0.05M CuCl, taking into account that 0.05M is a value close to the solubilization limit for copper (I) chloride in the DES.

3.1.1. Copper electrodeposition from Cu(I) solution

Cyclic voltammetry from Cu(I) solution shows that the peak associated to copper electrodeposition (Fig. 2A solid line) appears in the same potential range that that recorded previously from copper(II) solution. Also, reversing the scan at initio of the negative current the nucleation loop appeared (Fig. 2A dashed line). Positive scan was recorded till the peak associated to Cu(0) to Cu(I) oxidation appeared, avoiding Cu(I) to Cu(II) oxidation potential range.

On overlapping voltammetric curves for CuCl and $CuCl_2$ solutions at fixed concentration (0.05M) in DES (Fig. 2B), a good coincidence was found in the potential range associated to copper electrodeposition, confirming that the previous Cu(II)-Cu(I) reduction step doesn’t influence the electrodeposition mechanism.

The potentiostatic curves were recorded after applying a single-step signal from a potential at which no process occurs to those at which they do. All current transients exhibited the typical nucleation and three dimensional growth profile, current rising part that attains a maximum from which the current decays on increasing time (Fig. 3A). Comparing the curves obtained at different potentials evidences that maximum current (j_m) augments as the overpotential increases, while the time (t_m) at which appears shortens. Relatively high overpotentials were needed in order to observe relevant changes in rate of the process. It is worth noting that, for all potentials applied, the ends of the descending part do overlap so that applied potential does not affect the deposition process at long times. This induced us to calculate the Cu(I) diffusion coefficient in the DES, by linear logarithmic adjustment of the current vs time for each curve according to the well known Cotrell equation (Fig. 3A inset). Table 1 contains the different diffusion coefficient calculated averaging to $3.2 \cdot 10^{-7} cm^2 s^{-1}$. The values reproducibility shows that copper electrodeposition progresses via a 3D growth mechanism diffusion controlled.

Taking this into account, the chronoamperometric results were compared with those proposed by the model of Scharifker and Hills (S-H) [20,21]. This approach has been used extensively to analyse metal electrodeposition in aqueous media and lately has also in ionic liquid systems [22,23]. This model provides that, in non-dimensional form, instantaneous (all nuclei immediately formed after the step potential) and progressive nucleation (nuclei formed according to kinetics) follow respectively equations (1) and (2).

$$\left(\frac{j}{j_{\max}}\right)^2 = 1.9542\left(\frac{t}{t_m}\right)^{-1}\left[1-\exp\left(-1.2564\frac{t}{t_m}\right)\right]^2 \qquad (1)$$

$$\left(\frac{j}{j_{\max}}\right)^2 = 1.2254\left(\frac{t}{t_m}\right)^{-1}\left[1-\exp\left(-2.3367\left(\frac{t}{t_m}\right)^2\right)\right]^2 \qquad (2)$$

Comparison between the experimental j-t transients in the non-dimensional form and those corresponding to S-H model limit cases (Fig. 3B) did show that, at low overpotentials, the nucleation is nearly progressive, but upon increasing the overpotential intermediate nucleation was observed, tending to instantaneous behavior on increasing enough the overpotential. These results show that nucleation is activated by overpotential. The behavior observed for copper electrodeposition is quite different from that previously found at low temperatures from $CuCl_2$ solutions in the same medium [5]. Then, instantaneous nucleation followed by progressive one at long deposition times was proposed as justification. Nevertheless in our conditions, results obtained from the Cu(I) solution are in agreement with those usually expected, i.e. nucleation was favoured as the applied potential was made more negative.

In a parallel way, the logarithmic analysis of the rising part of the experimental j-t transients was made according to equations (3) and (4), derived assuming progressive and instantaneous nucleation respectively:

$$j = \frac{2}{3} zF\pi(2Dc)^{3/2} M^{1/2} \rho^{-1/2} N_o A t^{3/2} \tag{3}$$

$$j = zF\pi(2Dc)^{3/2} M^{1/2} \rho^{-1/2} N_o t^{1/2} \tag{4}$$

and where zF is the molar charge of the depositing species, D is the diffusion coefficient, c is the concentration, M is the molecular weight and ρ is the density, N_o is the maximum number of nuclei obtainable under the prevailing conditions and A is the steady state nucleation rate constant per site [20].

The adjustment was made for all the transients recorded (Fig. 4), except for those obtained at the highest overpotentials, in order to prevent the possible solvent reduction effect on the initial recorded current, which could interfere with the response and distort the analysis results. For the lowest overpotentials, calculated slopes were close to 1, whereas on increasing overpotential the slope tended to 0.5 as corresponds to instantaneous nucleation. This behaviour is in agreement with that obtained from the non-dimensional analysis via S-H model, in which a gradual transition from progressive nucleation to instantaneous was detected.

Since the nucleation mechanism for this kind of processes can also be derived using as evaluation tool the product $j_m^2 t_m$, these products were obtained for the complete series of experiments (Table 2). This approach requires that $j_m^2 t_m$ be equal to 1.94 10^{-6} A^2 cm^{-4} s and 1.22 10^{-6} A^2 cm^{-4} s for progressive and instantaneous nucleation respectively [20]. As can be seen in Table 2, at the lowest overpotentials the $j_m^2 t_m$ values correspond to intermediate behavior while at higher overpotentials the product approaches that predicted by instantaneous nucleation.

The results obtained from all the complementary analysis performed using the Cu(I) as electroactive species are congruent; the nucleation process evolves smoothly from progressive to instantaneous nucleation, in turn confirming also the applicability and the convergence of these treatments for copper deposition in the DES solutions.

3.1.2. Reduction of Cu(II) to Cu(I)

Cyclic voltammograms between 0.8 and -0.2 V were recorded at different scan rates from the $CuCl_2$ solution (Fig. 5A). The selected negative limit corresponds to a potential sufficiently far from the beginning of electrodeposition process. In the same manner that cyclic voltammetry from Figure 1 shows that the couple C_1/A_1 related to Cu(II)-Cu(I) reduction/oxidation has a similar profile that the corresponding to a reversible process. The differences $|E_{p,c}-E_{p,a}|$ between the potential peak of the cathodic peak (C_1) and the peak potential of the anodic peak (A_1) were determined (Table 3). These differences approach to 100mV at the lowest scan rates and increased as the scan rate increases. There is a significant difference between the expected (65 mV at 70ºC) and the obtained. This discrepancy was observed previously from experiments made at lower temperature (20ºC) and associated to resistance of organic media [5].

As the cathodic current peak versus the square root of potential scan rate plot was linear (Fig. 5B), the diffusion coefficient for the ion Cu(II) was calculated from the slope according to the equation [24]:

$$jp,c = 0.4463 * (\frac{F^3}{RT})10^5 * n^{3/2} * D^{\frac{1}{2}}[Cu(II)]v^{1/2} \qquad (5)$$

The resulting diffusion coefficient for the Cu(II) in the DES solvent at 70ºC was $4.67 \cdot 10^{-8}$ $cm^2 s^{-1}$, consistent with the previously reported value of $1.35 \cdot 10^{-8}$ cm^2 s^{-1} at 20ºC [5], taking into account the highest working temperature. It is remarkable that the Cu(I) diffusion coefficient calculated in the previous section was one order of magnitude higher than that obtained for Cu(II) species.

3.1.3 Copper electrodeposition from Cu(II) solution

In order to complete the copper electrodeposition study, the nucleation and growth process was analyzed using the $CuCl_2$ solution in the DES solvent.

In a first attempt, a series of j-t transients at different applied potential were recorded applying the typical single signal step, from an starting potential at which no process occurred to one at which Cu(II) reduction does. However, this procedure did not allow us to obtain reproducible j-t transients, whatever of the starting potential or the applied potential. This lack of reproducibility was attributed to the fact that Cu(II) reduction current adds to the Cu(I) electrodeposition response, so that the profile of the recorded j-t curve was the sum of two contributions, firstly Cu(II) reduction to Cu(I) and the subsequent Cu(I) electrodeposition. Thus, it was considered that the single-step potentiostatic procedure was unviable for this process, since several processeses are coupled on the current vs time response besides the copper electrodeposition. To simplify the problem new procedure was implemented.

As copper electrodeposition from Cu(II) solution takes place via preliminary Cu(II) - Cu(I) step, we decided to record the j-t transients by applying two consecutive steps. Starting from a potential (E_0) at which no process occurs, the potential was jumped to a potential value (E_1) in which only Cu(II) to Cu(I) can occur, such a value being maintained during a residence time (t_1). Afterwards, potential was switched to another potential value (E_2) at which copper electrodeposition takes place. The aim of this procedure is to maintain controlled conditions during the first step, thus allowing the second step (related to Cu(I) electrodeposition) to begin at fixed invariant conditions for all E_2 values employed, so that reproducibility is reached (Fig. 6A).

After an examination of the parameters involved in the strategy proposed, it was decided to fix E_0 at 0.6V and E_1 at -0.1V. Before recording the j-t curves, a systematic study was performed in order to evaluate how the residence time (t_1) at E_1 affects response. Thus, t_1 was varied from 1s to 50s while keeping the E_2 constant at -0.85V (Fig. 6B). The j-t profile obtained after this procedure shows two clear zones. At first, while potential E_1 is applied, the current monotonically decays (as corresponds to Cu(II) to Cu(I) reduction). On applying E_2, a current increase was observed that reaches a clear peak, followed by current decrease. The profile of the j-t transients during the second step is similar to that recorded using CuCl solution. Lastly, it is observed that on increasing t_1, a global decrease of the current involved in the second feature was observed, as corresponds to a decrease in the current associated to Cu (II) reduction. It is remarkable that, as the length pulse in E_1 was enlarged, much more decoupling between Cu(II)-Cu(I) reduction response and Cu(I) deposition is attained, allowing to identify peak profile much more clearly associated to Cu(I) deposition when E_2 is applied, an aspect of great importance for subsequent mechanistic analysis (Fig 6B). To confirm these observations, some series of experiments applying different E_2 were performed, in all cases, the observed behaviour being similar. From this previous examination it can be concluded that the decreasing contribution of Cu(II) reduction as the t_1 increases allows the identification of the j-t curve related to electrodeposition much more accurately. It should be noted however that diffusion of the Cu(I) species towards the solution is occurring simultaneously.

In view of the influence of the residence time t_1 on the profile of the transients associated to Cu(I) electrodeposition, at first, the j-t curves were recorded applying different E_2 potential values, maintaining t_1 at 5 seconds (Fig. 7A). This first t_1 value was selected considering both the contribution of Cu(II) reduction current changes and the Cu(I) diffusion to solution. Collecting the recorded transients at different E_2 potentials it was observed that increasing the overpotential sequentially, the current maximum increases and appears at shorter times. Comparing the descending parts of the curves recorded at E_2 at long deposition times the coincidence is not perfect but differences are not noteworthy.

Taking into account that copper electrodeposition works through a nucleation followed by 3D growth as it was demonstrated before, we aim to test if the S-H model, in the non dimensional plot could be applied as approximation to study nucleation mechanism from the data recorded during the second potentiostatic step from the $CuCl_2$ solution, taking advantage from the fact that non-dimensional equations does not contain concentration electroactive species dependence.

Previously to the application of the S-H model, current related to Cu(II) reduction must be subtracted from global current recorded in order to remove this additional current contribution. Thus, it was recorded the j-t transient corresponding to Cu(II)-Cu(I) reduction during 40s, time sufficient to cover the time range corresponding to the application of E_2 studied.

The non-dimensional adjustment of the curves j-t obtained after a 5s residence time t_1 is plotted in figure 7B. It can be seen that non-dimensional curves from experimental data obtained applying this double-step potentiostatic signal fit quite well with the S-H model allowing, in principle, some predictions about the nucleation-growth mechanism of the process to be made. However, from non-dimensional adjustment it is also observed that nucleation mechanism tends to instantaneous behavior reaching it at a not really high applied overpotential contrasting with non-dimensional analysis results electrodepositing copper directly from Cu(I) solution (Figure 3B). This could mean that after t_1=5s nucleation is overestimated. Moreover, when an analysis of the rising part of the j-t transients is performed, no coherent correlation is found with that obtained from Cu(I) solution. Therefore, it is clear that not sufficiently accurate estimation of the nucleation mechanism can be achieved by selecting a 5s residence time in potential E_1, although it fit curves j-t to S-H model.

In view of the above exposed facts, to further refine the results, it was decided, after revising the experimental results shown in Fig 7A for the current related to Cu(II) reduction at Cu(I) (dashed line), to record j-t curves increasing the residence time in E_1, to 10s. The objective was to minimize the change in overall recorded current along deposition time, associated to the Cu(II) reduction to Cu(I). The current associated from Cu(II) to Cu(I) reduction hardly changes at all after the time-range selected. These changes may distort the extracted current of electrodeposition process especially at the low deposition times. This selected residence time also has the risk of losing part of the Cu(I) but due to the quantitative treatment characteristics this does not constitute a dramatic variable.

Figure 7C shows j-t curves at different applied potentials E_2. The observed behavior is analogous to that shown in figure 7A but now, comparing the descending parts of the transients, much better overlapping of the curves was obtained, spite of the double step signal applied, as corresponds to 3-D growth diffusion-controlled. The j-t curves profiles are in agreement with suppositions made above.

When these new j-t curves were adjusted to the non-dimensional S-H equations (Fig. 7D) it was observed that at the lower overpotentials analyzed the nucleation follows an intermediate mechanism which tends to instantaneous one increasing progressively and sufficiently the overpotential. The comparison of the results with those obtained from the CuCl solution shows that now the behavior coincidence observed is better than the obtained previously using lower t_1.

The analysis of the corresponding rising parts of the experimental j-t curves recorded applying the potential E_2 is in agreement with the non-dimensional analysis, and congruent with the previously obtained from the CuCl solution. The obtained slopes approach to 0.5 upon increasing the overpotential, as correspond to the evolution to an instantaneous mechanism (Fig. 8). Comparing, at fixed potential, the slope values obtained for the rising parts of the copper electrodeposition j-t transients recorded from the two solutions, CuCl and $CuCl_2$, little differences between the values are observed.

This satisfactory concordance in the obtained results from CuCl and $CuCl_2$ solutions using the proposed strategy provides an useful tool that may allow the accurate analysis of electrodeposition processes in which the intermediate valences are sufficiently stabilized in the plating solution as it is this case of Cu(I) in chloride medium. The use of a double step procedure allows to assure that the Cu(I) presence near the electrode when the electrodeposition process starts is similar in all conditions. Although at these conditions, the Cu(I) concentration is unknown due to the different diffusion fluxes, it is expected that, in all experiments, the initial conditions for the subsequent step are similar, as the first jump conditions are fixed, procedure that facilitates the reproducibility and coherence of the response at the different E_2 applied. Moreover, in DES, the extension of the length of the first pulse improves the results, allowing the accuracy of the analysis because the current recorded at these conditions is less sensitive to the changes associated to the Cu(II) reduction.

Therefore, the characteristics of the response recorded by double step procedure when the electrodeposition process involves nucleation followed by 3D growth diffusion controlled, permits the evaluation of the data, using as acceptable approaching the non-dimensional equations derived from SH model and the rising part analysis. This experimental method has been demonstrated useful when the stabilization of intermediate species by the reaction medium takes place, as occurs for Cu(I) in chloride medium. The stabilization of species leads to sufficient separate reduction processes, as the manner that when potentiostatic experiments were performed by means a single step, the response is disturbed by the contribution of outside currents to the electrodeposition process and leads to no coherent results, when they adjust to theoretical models.

3.2. Copper electrodeposition in aqueous chloride medium

As it is well known, in chloride medium, copper reduction from Cu(II) also occurs in two steps sufficiently separated due to the stabilization of copper (I) by formation of complexes with chloride [25]. Now we focused our efforts in the study of the copper deposition process in concentrated chloride aqueous medium, in order to establish the effect of chloride presence in the overall deposition process.

The potential range at which copper reduction occurs in 0.01M $CuCl_2$ and 0.01M CuCl both plus 3M NaCl solutions was established by cyclic voltammetry (Fig. 9). The concentration of 3M NaCl was needed to ensure total solubilization of the Cu(I) by complexation [26]. As was expected, the cyclic voltammetry for Cu(II) showed two groups of features: first one corresponding to Cu(II)-Cu(I) reduction/oxidation reversible process, and the second group corresponding to Cu(I) electrodeposition. In aqueous medium the potential range at which the processes occur is sited at more positive potentials than in DES solvent, highlighting that aqueous medium favors deposition even at this concentrated chloride presence. A good coincidence in the potential range at which electrodeposition takes place was found overlapping the voltammetric curves recorded from CuCl and $CuCl_2$ solutions suggesting that, as occurs in DES solvent, Cu(II) reduction does not influence the mechanism of the electrodeposition of Cu(I). Moreover, the voltammetric peak associated to copper electrodeposition shows a sharper current increase than the corresponding detected on DES and a well defined maximum, features that confirms the more favored deposition process in aqueous medium.

From the $CuCl_2$ solution and restricting the voltammetric negative limit to potentials at which only Cu(II)-Cu(I) reduction/oxidation occurs cyclic voltammograms were recorded different scan rates (Fig. 10A) and the Cu(II) diffusion coefficient was calculated plotting each recorded current versus $v^{1/2}$. Good linearity (Fig. 10B) was obtained, being the calculated diffusion coefficient $3.67 \cdot 10^{-6}$ cm^2s^{-1}, value in accordance with those obtained for Cu(II) in sulphate aqueous medium [7].

3.2.1. *Copper electrodeposition from Cu(I) solution*

First stages of copper electrodeposition mechanism in rich-chloride aqueous media were analyzed, firstly, using the solution containing CuCl by means potentiostatic method. The j-t curves from 0.01M CuCl plus 3M NaCl solution recorded applying single potential step are shown in (Fig. 11A). The j-t transients show the typical profile of nucleation process followed by 3D growth controlled by diffusion. It is worthy to mention that in aqueous medium is needed a narrow potential range to observe relevant changes in the recorded j-t transients. At longer times, the recorded curves overlap, confirming the diffusion control for the electrodeposition process. The diffusion coefficient calculated (Table 1) by Cotrell's equation and using the ending of the descending curves, averages $1.5 \cdot 10^{-5} cm^2s^{-1}$. This value is higher than that for Cu(II) and also fifty times higher than that calculated for Cu(I) in DES, a fact attributable to the species greater mobility in aqueous medium.

The potentiostatic curves obtained from the CuCl solution adjusted to non-dimensional S-H model showed that, in the analyzed potential range, copper electrodeposition works through an intermediate mechanism and tends to instantaneous one when overpotential was increased (Fig. 11B). In this aqueous medium, the gradual change occurs in a shorter potential range than in DES media. This approach to instantaneous behavior was also supported by the results provided by the complementary logarithmic analysis of the rising part of the experimental j-t transients. Linear dependence was obtained (Fig. 12A), and the calculated slopes tend to 0.5, although is not achieved, increasing the overpotential as predict equation (4) for instantaneous nucleation. The nucleation type derived from the j_m and t_m values by means the criteria j_m^2 x t_m confirms the intermediate behavior (Table 2), with transition to progressive to instantaneous nucleation. The calculated products at the higher overpotentials tested approach to the predicted for instantaneous nucleation (j_m^2 x t_m = 2.28*10^{-6} A^2 cm^{-4} s), whereas the lower are far of the predicted by progressive (j_m^2 x t_m = 3.63*10^{-6} A^2 cm^{-4} s).

Thus, from these experiments, it is confirmed the applicability of the S-H model to analyze the nucleation mechanism from rich-chloride aqueous solution containing CuCl. Both the non-dimensional adjustment and the logarithmic analysis of the rising part of the j-t transients supported that copper electrodeposition tends to instantaneous mechanism increasing the overpotential.

3.2.2. Copper electrodeposition from Cu(II) solution

As occurred in DES, it was not possible obtaining reproducible results applying single potentiostatic step using solutions containing Cu(II) in chloride excess. In this section our efforts addressed testing the applicability of the developed two step potential protocol to the first stages study of copper nucleation and 3D growth mechanism in aqueous medium. For this purpose 0.01M $CuCl_2$ plus 3M NaCl solution was used.

After a deep analysis of the applied potential effect, it was decided to fix E_0 at 0.8V and E_1 at 0V, being the latter enough separated from Cu(I) electrodeposition, ensuring that only Cu(II)-Cu(I) reduction occurs at this first step.

It was firstly evaluated as Cu(II)-Cu(I) reduction influences the electrochemical response related to copper electrodeposition, recording j-t curves keeping E_1 and E_2 constant and increasing progressively the residence time (t_1) in $E_{1,}$ t_1 was varied between 0.5 and 5s attending the foreseeable high mobility of ion species in aqueous medium. The recorded transient shows two clear zones, the corresponding to the reduction of Cu(II) to Cu(I) and that of copper electrodeposition. Taking into account that these diffusion coefficients of both Cu(II) and Cu(II) in aqueous solution are considerably higher than those obtained in DES, it was decided to fix residence time (t_1) in 1s for using the double step signal (ten times lower than that used in the DES solvent). This residence time is a compromise value with the purpose to minimize both the decrease of Cu(I) concentration on the electrode surface and the contribution to overall current of Cu(II) reduction. Low residence time implies higher contribution of Cu(II)-Cu(I) reduction process, making it difficult to extract electrodeposition current without error. Enlarging t_1 favors the Cu(I) diffusion to the solution.

The profile for all j-t curves recorded at different E_2 (Fig. 13A) shows the characteristic profile corresponding to a nucleation followed by 3-D growth. Reproducibility was getting very hard. Comparing the descending parts of the j-t transients overlapping at high deposition time was found.

However contrasting with that observed when Cu(I) was directly electrodeposited, at these conditions low E_2 values were necessary to increase the deposition rate, value of 600 mV was applied. This fact could be related to low Cu(I) concentration on the electrode surface due to the favored diffusion towards the solution. The decrease of electroactive species on the surface would explain the low current response compared with that obtained at fixed potential from the Cu(I) solution in aqueous solution.-

The j-t transients obtained at different E_2 potential values were fitted to the non-dimensional equations provided by S-H model, after subtracting the corresponding Cu(II) to Cu(I) reduction current in the overall recorded current. Non-dimensional adjustment (Fig. 13B) shows that mechanism corresponds to intermediate behavior at the lower applied potentials, and as occurs from the Cu(I) solution, increasing the overpotential, the curves approach to that corresponding to instantaneous mechanism. In the same way, the analysis of the rising part of the curves supports these results, the slope values of the linear representation (Fig. 12B) progressively decrease, approaching to values near to 0.5, limit of instantaneous nucleation.

The results indicate that as occurs in DES solvent, from $CuCl_2$ aqueous solution in chloride excess also the S-H model could be applied, as approximation, to study the nucleation mechanism fitting the j-t transients recorded during the second stretch of the double step procedure, decreasing the residence time t_1. But spite of low residence time, attain reproducibility is hard, the mobility of the ionic species in aqueous medium makes difficult to keep control of the initial conditions, due to Cu(I) diffuses easily to the solution. Thus, in aqueous medium, the diffusion rate limits the application of this procedure, forcing applying high overpotentials to obtain a significant current response, although overcoming the experimental drawbacks it was demonstrated that reliable information about the nucleation process is obtained.

The general behavior is in concordance with that obtained from mechanistic analysis from the CuCl solution using single step signal. So, the consistency of the mechanistic results obtained from both $CuCl_2$ and CuCl solutions supports the usefulness of the double step signal protocol proposed, taking care that the residence time is well selected depending on the particular characteristics of the medium.

3.3. Morphological characterization of copper deposits

In order to analyze how the nature of the solvent could affect the growth of copper electrodeposits, a morphological analysis was performed both in DES and in aqueous media. Figure 14 A shows that, when deposit was prepared from the DES solution, a population of small grains with characteristic morphology appeared suggesting low superficial diffusion and difficult nucleation at the low overpotentials. Increasing both the overpotential and the applied charge, population of grains, that shows similar morphology, increases (Fig. 14 B). Although coalescence is not achieved some dendritic growth was observed at high overpotential.

On the other hand, when deposits were prepared in the aqueous solution with excess of chloride, blocks much bigger appear (Fig. 14 C). In this medium, higher superficial diffusion in the vitreous carbon allows the higher aggregation of the nucleus formed, leading to crystals of high size. However, a detailed analysis of the SEM pictures indicates that the morphology of the deposits is no affected by the medium, similar morphology was obtained regardless of whether the deposit was formed in the DES or in the chloride medium.

To verify if morphology is affected by the presence of chloride, copper was electrodeposited from $NaClO_4$ 0.5M plus $CuCl_2$ 0.01M solution at different potentials. Copper electrodeposition occurs faster in perchlorate than in chloride medium.

Figure 14 D shows that the deposit prepared in perchlorate medium at low overpotential is formed by blocks which size is comparable to those obtained in chloride aqueous medium at similar charge although at difference than those obtained in chloride medium, the grains are less smoother and show more complex morphology. In this medium, when the deposits were prepared rising slightly the overpotential, it was observed that the deposit is constituted by crystals, all of them of similar size, suggesting that in perchlorate medium copper electrodeposition easily takes place through an instantaneous mechanism (Fig. 14 E).

All these results suggest that copper electrodeposition takes place through a mechanism which approach to instantaneous behavior, easily in perchlorate medium and slowly in chloride one. The chloride presence seems to delay slightly dendrite appearance as deduced in the comparison between the deposits obtained from perchlorate and chloride in aqueous medium. The lower diffusion superficial in DES results in a homogenous distribution of grains with size smaller than the observed in chloride media although morphology does not seem affected dramatically by DES.

4. Conclusions

This work reports mechanistic analysis of the copper electrodeposition from a eutectic mixture of choline chloride-urea. The electrochemical reduction was studied by cyclic voltammetry and the nucleation and growth process was investigated by potentiostatic technique. Similar analysis was made in aqueous solution with excess chloride ion.

Both chronoamperometric and voltammetric results make in evidence that the copper deposition in all conditions studied corresponds to a nucleation and 3D growth process, diffusion controlled.

The use of DES as solvent slows the growth process. In the DES solvent higher both temperature and concentration are needed in order to attain current comparable with the obtained in aqueous medium.

The applicability of the S-H model in the DES solvent was demonstrated, making in evidence that copper deposition approaches to instantaneous nucleation applying sufficient overpotentials.

It was designed a two step potential procedure to study the nucleation mechanism when copper reduction takes place from Cu(II) solutions in two steps sufficiently separated, involving each one the transference of one electron. The applicability of the S-H model has been demonstrated for the transients obtained along the second step. The fact that S-H non-dimensional equations do not depend on the concentration allows the use of the model. The requirement is to keep controlled the initial conditions of second step; this is achieved by properly selecting of residence time in the first step.

In conclusion, the double step signal proposed can be applied successfully to study the electrodeposition process when intermediate species are stabilized by species present in the media, being the procedure success dependent on the control of the initial conditions at which electrodeposition takes place. In DES the low mobility of species facilitates the application of the procedure, whereas in aqueous medium the great mobility of ionic species makes difficult it.

This strategy does not allow to estimate Cu(I) concentration on the surface. The perspective for the future would be focused on finding the appropriate model which could describe accurately processes which involve more than one electroreduction step and provide the complete mechanistic parameters to understand this kind of electrodeposition processes. More work in this field is stell needed to be performed.

Finally, the morphological study demonstrates neither chloride presence nor DES solvent affect significantly the morphology of final deposits although a smoothness of the grains was observed. The small size of the grains obtained in DES by comparing them with those obtained in aqueous medium, confirms the lower superficial diffusion in DES. The uniformity of the grain size in perchlorate medium at moderate overpotentials confirms copper electrodeposition mechanism tends to instantaneous condition.

Acknowledgements

Financial support from the *MINECO* contract CTQ2010-20726 (subprogram BQU) is grateful acknowledged. The authors wish to thank the *Centres Científics i Tecnològics de la Universitat de Barcelona (CCiTUB)* for the use of their equipment.

References

[1] C.K. Hu, J.M.E. Harper, Mater. Chem. Phys. 52 (1998) 5-16.

[2] A. Ramos, M. Miranda-Hernández, I. González, J. Electrochem. Soc. 148 (2001) C315-C321.

[3] D. Grujicic, B. Pesic, Electrochim. Acta, 2002, 47, 2901-2912.

[4] D. Grujicic and B. Pesic. Electrochim. Acta, 2005, 50, 4426-4443.

[5] A.P. Abbott, K. E. Tabib, G. Frisch, K. J. Mckenzie, K. S. Ryder, Phys. Chem. Chem. Phys. 11 (2009) 4269-4277.

[6] M.R. Majidi, K. Asadpour-Zeynali, B. Hafezi, Electrochim. Acta 54 (2009) 119-1126.

[7] M. Gu and Q. Zhong, J. Appl. Electrochem. 41 (2011) 765-771.

[8] Electrochemical Aspects of Ionic Liquids, Ed. Hiroyuki Ohno, John Wiley & Sons, 2005 New Jersey.

[9] A.P. Abbott, G. Capper, D.L. Davies, R.K. Rasheed, P. Shikotra, Inorg. Chem. 44 (2005) 6497-6499.

[10] S. Salomé, N.M. Pereira, E.S. Ferreira, C.M. Pereira, A.F. Silva, J. Electroanal.Chem. 703 (2013) 80-87.

[11] J.C. Malaquias, M. Steichen, M. Thomassey, P.J. Dale, Electrochim. Acta 103 (2013) 15-22.

[12] P. Guillamat, M. Cortes, E. Valles, E. Gomez, Surf. Coat. Technol. 206 (2012) 4439-4448.

[13] K. Haerens, E. Matthijs, A. Chmielarz, B.V. Bruggen., J. Environmental. Management 90 (2009) 3245-3252.

[14] L.A. Woolf, A. W. Hoveling, J. Phys. Chem. 74 (1970) 2046-2048.

[15] L-Bonou, M. Eyraud, J. Crousier, J. Appl. Electrochem. 24 (1994) 906-910.

[16] C. A. Gunawan, B. H. R. Suryanto, C. Zhao, J. Electrochem. Soc. 159 (2012) D611-D615.

[17] M. A. Pasquale, L. M. Gassa, A. J. Arvia, Electrochim. Acta 53 (2008) 5891-5904.

[18] E.P. Grishina, A.M. Pimenova, N.O. Kudryakova, L.M. Ramenskaya, Russ. J. Electrochem. 48(12) (2012) 1166-1170.

[19] E. Gomez, P. Cojocaru, L. Magagnin and E. Valles, J. Electroanal. Chem. 658 (1-2) (2011) 18-24

[20] G. Gunawardena, G. Hills, I. Montenegro, B. Sharifker, J. Electroanal. Chem. 138 (1982) 225-239.

[21] B. Scharifker, G. Hills, Electrochim. Acta 28 (1983) 879-889.

[22] O. Mann, W. Freyland. J. Phys. Chem. C 111 (2007) 9832-9838.

[23] T. Jiang, M.J. Chollier, Brym, G. Dube, A. Lasin, G.M. Brisard, Surf. Coat. Technol. 201 (2006) 10-18.

[24] A. A. F. Bard and R. Larry. Electrochemical methods: fundamentals and applications, page 231, 2nd ed., John Wiley & Sons Inc., New York, 1980.

[25] G. Gunawardena, G. Hills, I. Montenegro. J. Electroanal. Chem. 184 (1985) 357-369.

[26] MEDUSA-Chemical Diagrams (2.0) and HYDRA-Hydrochemical Database (2.0). Softwares of I. Puigdomenech. http://www.kemi.kth.se/medusa/.

Captions for Figures

Fig. 1. Voltammetric curves at 50 mVs^{-1} from 0.05 M $CuCl_2$ in DES solvent at different negative limits: solid line) -1500mV and dashed line) -770mV.

Fig. 2. Voltammetric curves at 50 mVs^{-1} from A) 0.05 M CuCl in DES solvent at different negative limits: solid line) -1500mV and dashed line) -847mV. B) solid line) 0.05 M $CuCl_2$ in DES solvent and dashed line) 0.05M CuCl in DES solvent.

Fig. 3. A) Potentiostatic current transients from 0.05M CuCl in DES solution, curves a) -750 b) -800, c) -850, d) -900, e) -965, f) -1000 and g) -1065 mV. Inset: Plots according Cotrell equation for curves d, f and g. B) Non-dimensional plots of $(j/j_m)^2$ vs t/t_m for some of j-t transients of figure 3A.

Fig. 4. Current vs time, logarithmic plot of rising part of the current transients for the deposition of copper from 0.05M CuCl in DES solvent, curves: a) -750, b) -800, c) -850, d) -900, e) -965 and f) -1000 mV.

Fig. 5. A) Voltammetric curves at different scan rates from $CuCl_2$, 0.05M in DES solvent from 0.800V to -0.200V curves: a) 5, b) 10, c) 20, d) 50, e) 100, f) 150 and g) 200 mV/s. B) Corresponding $j_{p,c}$ vs $v^{1/2}$ plot.

Fig. 6. A) Scheme of the applied signal to record j-t transients. B) Potentiostatic current transients from 0.05M $CuCl_2$ in DES solvent using double step signal, E_1= -100 mV E_2= -850 mV and different residence times (t_1): a) 1 b) 5, c) 10, d) 20, e) 50 and f) 60s.

Fig. 7. A) Potentiostatic current transients for the deposition of copper from 0.05M $CuCl_2$ in DES solvent, using double step signal, E_1= -100 mV t_1= 5s- and different E_2: a) -800, b) -850, c) -950, d) -1000, e) -1050, f) -1075, g) -1100 and h) 1150 mV. B) Non-dimensional plots of $(j/j_m)^2$ vs t/t_m for some of j-t transients of figure 7A. C) Same solution and conditions and t_1= 10s at different E_2: a) -800, b) -850, c) -900, d) -950, e) -1000. B) Non-dimensional plots of $(j/j_m)^2$ vs t/t_m for some of j-t transients of figure 7C.

Fig. 8. Current vs time, logarithmic plot of rising part of the j-t transients of Figure 7C, at E_2: a) -850, b) -900, c) -950 and d) -1000 mV.

Fig. 9. Voltammetric curves in aqueous medium at 50 mVs^{-1} from: solid line) 0.01 M $CuCl_2$ + 3M NaCl, dashed line) 0.01M CuCl + 3M NaCl.

Fig. 10. A) Voltammetric curves in aqueous medium at different scan rates from 0.01M $CuCl_2$ +3M NaCl solution, scanning between 0.6V and -0.1V: a) 5, b) 10, c) 20, d) 50, e) 100, f) 150 and g) 200 mV/s. B) Corresponding j vs $v^{1/2}$ plot.

Fig. 11. A) Potentiostatic current transients for the deposition of copper from 0.01M CuCl + 3M NaCl solution, curves: a) -345, b) -355, c) -360, d) -375, e) -390, f) -400 and g) -415 mV. B) Non-dimensional plots of $(j/j_m)^2$ vs t/t_m for some of j-t transients of figure 11A.

Fig. 12. Current vs time, logarithmic plot of rising part of the j-t transients: A) from 0.01M CuCl + 3M NaCl solution at: a) -355, b) -375, c) -400 and d) -415 mV. B) from 0.01M $CuCl_2$+ 3N NaCl, using double step signal at: a) -400, b) -450, c) -500 and d) -550 mV.

Fig. 13. A) Potentiostatic current transients for the deposition of copper from 0.01M $CuCl_2$+ 3N NaCl, using double step signal, E_1= 0 mV t_1= 1s and different E_2: a) -400, b) -450, c) -500, d) -520, e) -550, f) -600 and g) -650mV. B) Non-dimensional plots of $(j/j_m)^2$ vs t/t_m for some of j-t transients of figure 13A.

Fig. 14. SEM images of deposits prepared potentiostaticaly from different solutions: 0.05M de CuCl in DES solvent at: A) -850 mV, Q= -10 mC and B) -870 mV, Q=30 mC; C) 0.01M CuCl + NaCl 3M solution at -300 mV, Q=20 mC, and 0.01M CuCl + 0.6M $NaClO_4$ solution at: D) -100 mV, Q= 15 mC and E) -115 mV, Q= 15 mC.

Table 1.

Diffusion coefficients obtained from the descending part of the j-t transients in the analyzed solutions

3M NaCl		DES Solvent	
[Cu(I)]=0.01 M		[Cu(I)]=0.05 M	
E/mV	D/cm^{2}s^{-1}	E / mV	D/cm^{2}s^{-1}
-415	1.50E-05	-1065	3.27E-07
-400	1.47E-05	-1000	3.14E-07
-390	1.51E-05	-965	3.06E-07
-375	1.41E-05	-900	3.22E-07

E vs (Ag/AgCl)

Table 2.

Characteristics of the potentiostatic current maximum for the j-t transients obtained from [Cu(I)]=0.05M in DES solvent and [Cu(I)]=0.05M + [NaCl]=0.01M in aqueous medium

	E/mV	t_m/s	j_m/A cm^{-2}	$j_m^2\ t_m$
DES solvent [Cu(I)]=0.05M	-750	9.81	-0.41E-3	1.64E-06
	-800	4.66	-0.57E-3	1.52E-06
	-850	2.86	0.73E-3	1.51E-06
	-900	2.01	-0.85E-3	1.45E-06
	-965	1.56	-0.95E-3	1.42E-06
	-1000	0.99	-1.20E-3	1.42E-06
Chloride 3M [Cu(I)]=0.01M	-355	2.645	-0.98E-3	2.53E-06
	-360	1.775	-1.22E-3	2.62E-06
	-375	1.085	-1.54E-3	2.57E-06
	-390	0.605	-2.09E-3	2.65E-06
	-400	0.435	-2.45E-3	2.61E-06

E vs (Ag/AgCl)

Table 3.

Characteristic values of $E_{p,c}$ and $j_{p,c}$ for the cathodic peak and $E_{p,a}$ and $j_{p,a}$ for the anodic peak at different scan rates in the analyzed solutions.

	v / mV s^{-1}	E_{pc} / V	E_{pa} / V	lE_{pc}-E_{pa}l / V
DES solvent [Cu(II)]=0.05M	200	0.239	0.434	0.185
	150	0.239	0.422	0.173
	100	0.239	0.422	0.173
	50	0.241	0.412	0.161
	20	0.272	0.389	0.117
	10	0.275	0.387	0.112
	5	0.278	0.383	0.105
Chloride 3M [Cu(II)]=0.01M	200	0.295	0.383	0.078
	150	0.295	0.388	0.073
	100	0.288	0.383	0.075
	50	0.297	0.373	0.076
	20	0.307	0.378	0.071
	10	0.305	0.378	0.073
	5	0.305	0.375	0.071

E vs (Ag/AgCl)

Table 1.

Diffusion coefficients obtained from the descending part of the j-t transients in the analyzed solutions

3M NaCl		DES Solvent	
[Cu(I)]=0.01 M		[Cu(I)]=0.05 M	
E/mV	D/cm^{2}s^{-1}	E / mV	D/cm^{2}s^{-1}
-415	1.50E-05	-1065	3.27E-07
-400	1.47E-05	-1000	3.14E-07
-390	1.51E-05	-965	3.06E-07
-375	1.41E-05	-900	3.22E-07

E vs (Ag/AgCl)

Table2

Table 2.

Characteristics of the potentiostatic current maximum for the j-t transients obtained from [Cu(I)]=0.05M in DES solvent and [Cu(I)]=0.05M + [NaCl]=0.01M in aqueous medium

	E/mV	t_m/s	j_m/A cm^{-2}	$j_m^2\ t_m$
DES solvent [Cu(I)]=0.05M	-750	9.81	-0.41E-3	1.64E-06
	-800	4.66	-0.57E-3	1.52E-06
	-850	2.86	0.72E-3	1.51E-06
	-900	2.01	-0.85E-3	1.45E-06
	-965	1.56	-0.95E-3	1.42E-06
	-1000	0.99	-1.20E-3	1.42E-06
Chloride 3M [Cu(I)]=0.01M	-355	2.645	-0.98E-3	2.53E-06
	-360	1.775	-1.22E-3	2.62E-06
	-375	1.085	-1.54E-3	2.57E-06
	-390	0.605	-2.09E-3	2.65E-06
	-400	0.435	-2.45E-3	2.61E-06

E vs (Ag/AgCl)

Table 3.

Characteristic values of $E_{p,c}$ and $j_{p,c}$ for the cathodic peak and $E_{p,a}$ and $j_{p,a}$ for the anodic peak at different scan rates in the analyzed solutions.

	v / mV s^{-1}	E_{pc} / V	E_{pa} / V	lE_{pc}-E_{pa}l / V
DES solvent [Cu(II)]=0.05M	200	0.239	0.434	0.185
	150	0.239	0.422	0.173
	100	0.239	0.422	0.173
	50	0.241	0.412	0.161
	20	0.272	0.389	0.117
	10	0.275	0.387	0.112
	5	0.278	0.383	0.105
Chloride 3M [Cu(II)]=0.01M	200	0.295	0.383	0.078
	150	0.295	0.388	0.073
	100	0.288	0.383	0.075
	50	0.297	0.373	0.076
	20	0.307	0.378	0.071
	10	0.305	0.378	0.073
	5	0.305	0.375	0.071

E vs (Ag/AgCl)

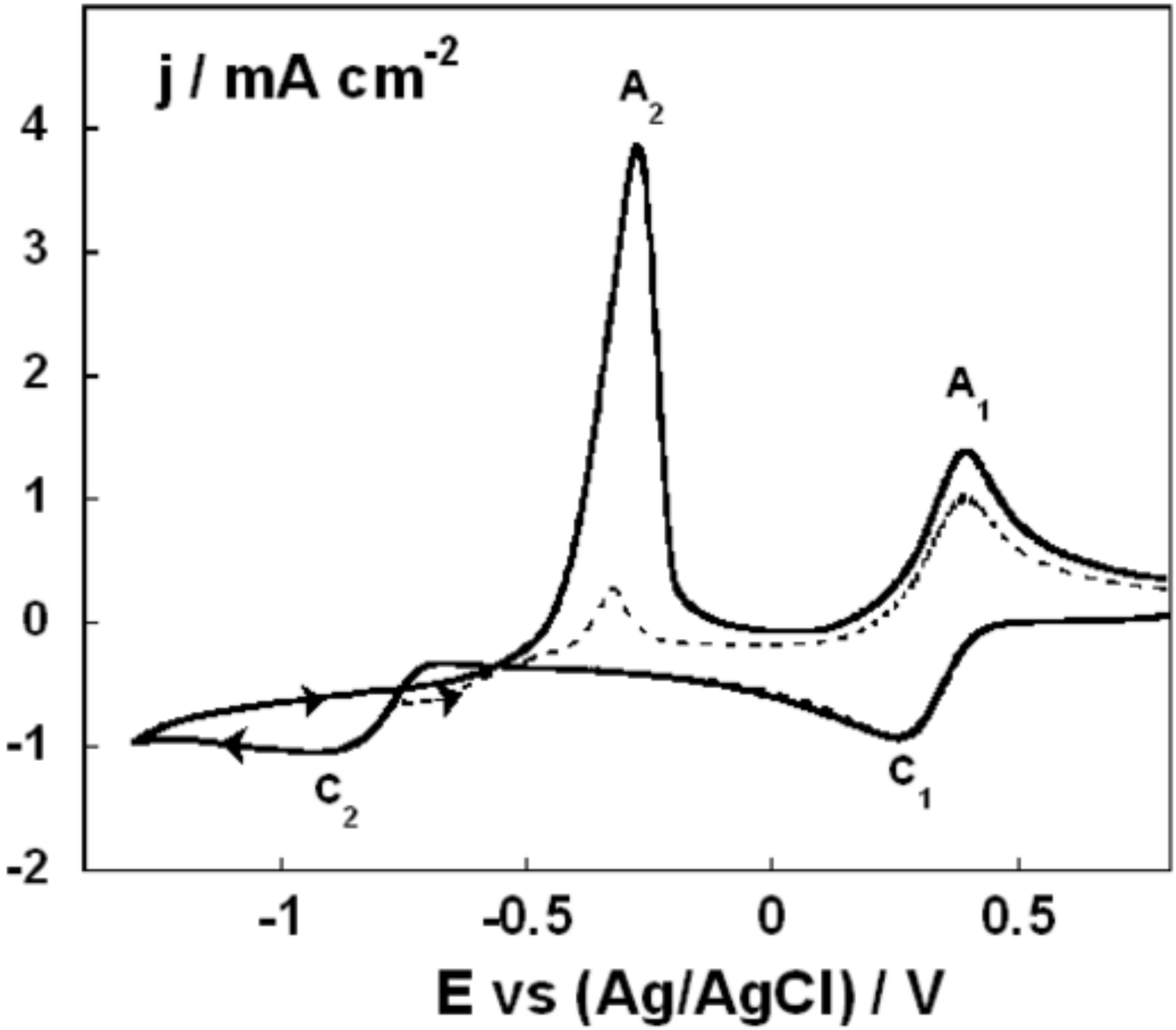

Figure 1

Figure2

Click here to download high resolution image

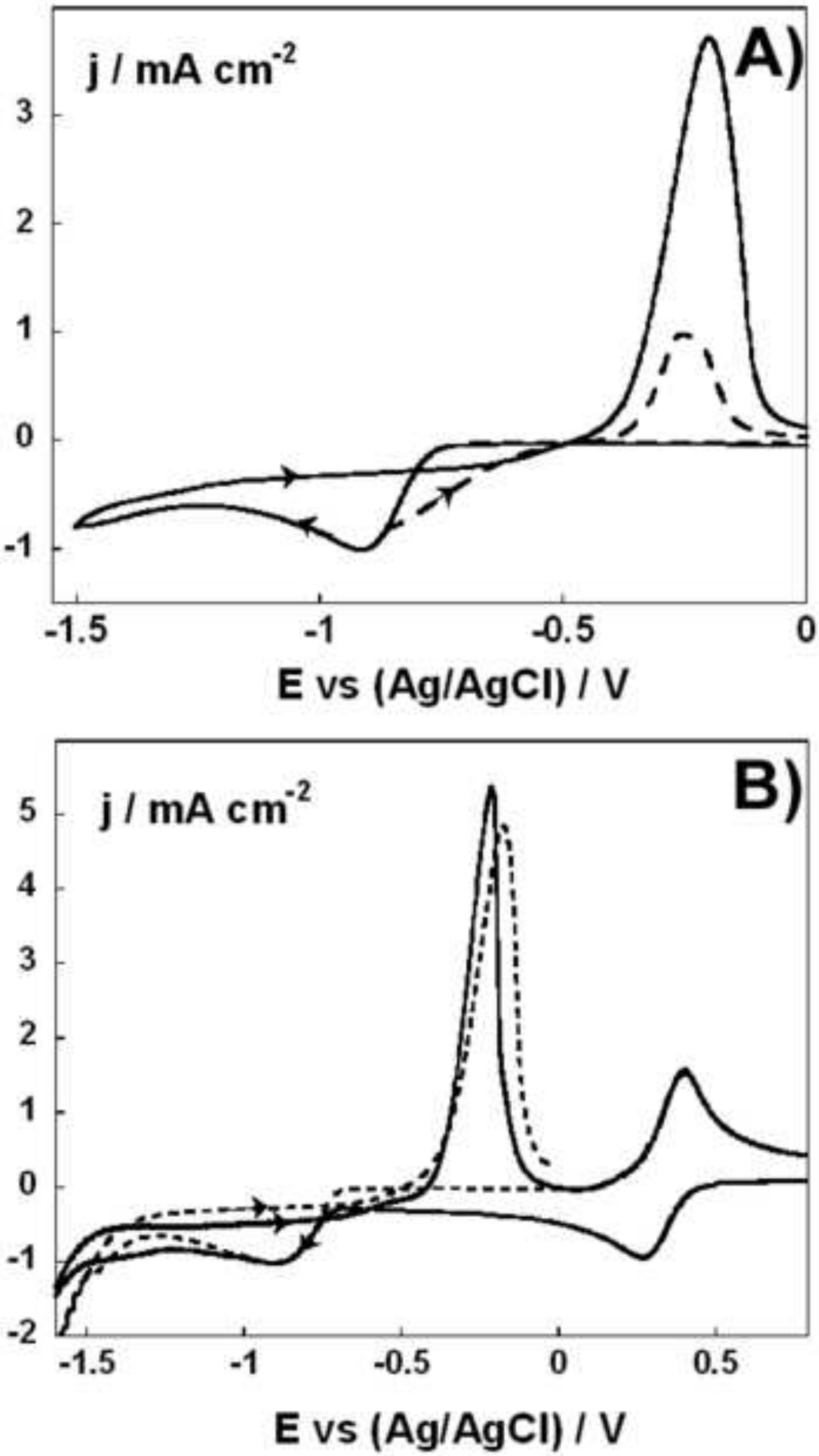

Figure 2

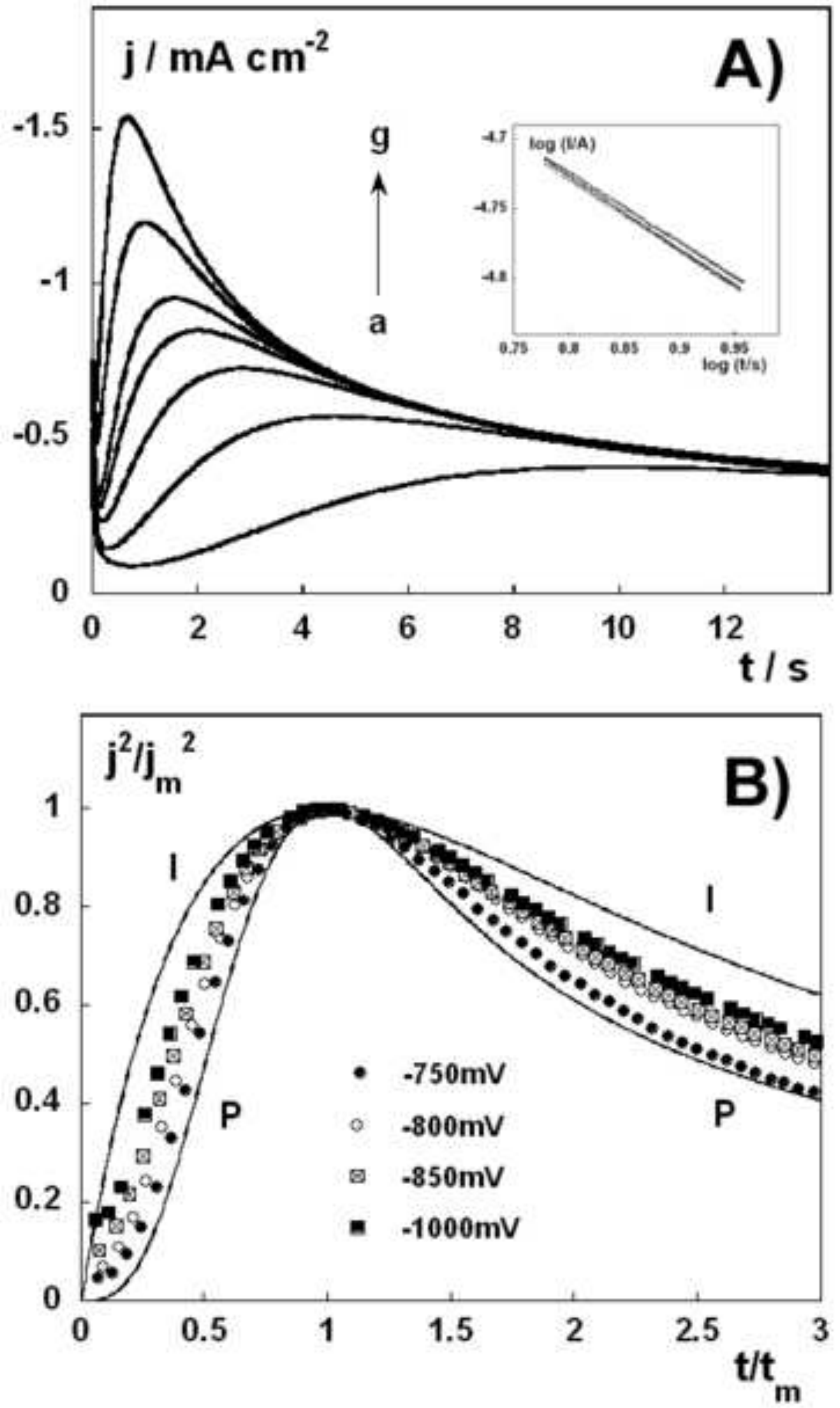
j / mA cm^{-2}
A)
-1.5
-1
-0.5
0
g
a
0
2
4
6
8
10
12
t / s
-4.7
-4.75
-4.8
log (I/A)
0.75
0.8
0.85
0.9
0.95
log (t/s)
j^2/j$_m$^{2}
B)
1
0.8
0.6
0.4
0.2
0
I
P
I
P
● -750mV
○ -800mV
⊠ -850mV
■ -1000mV
0
0.5
1
1.5
2
2.5
3
t/t$_m$

Figure 3

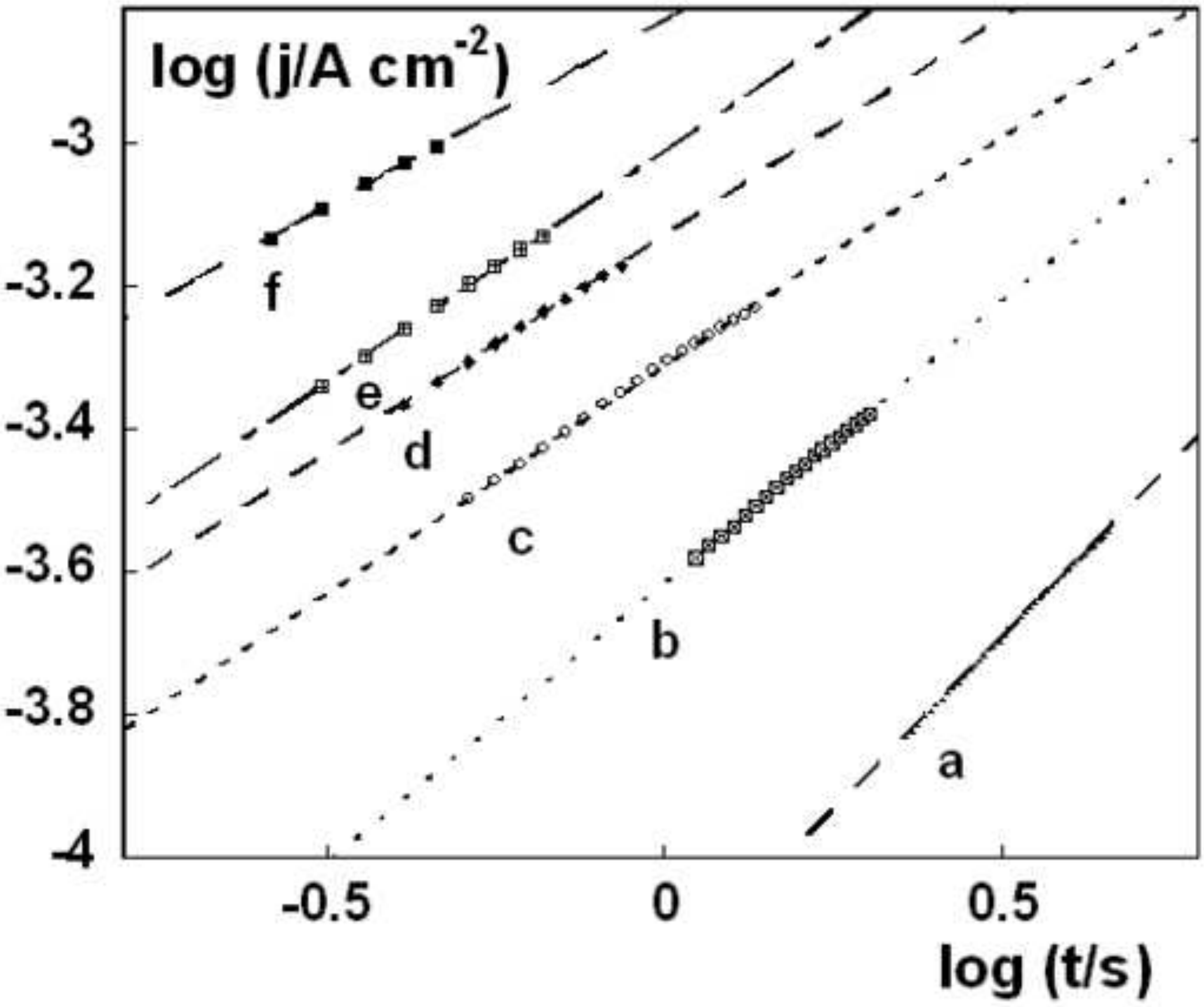

Figure 4

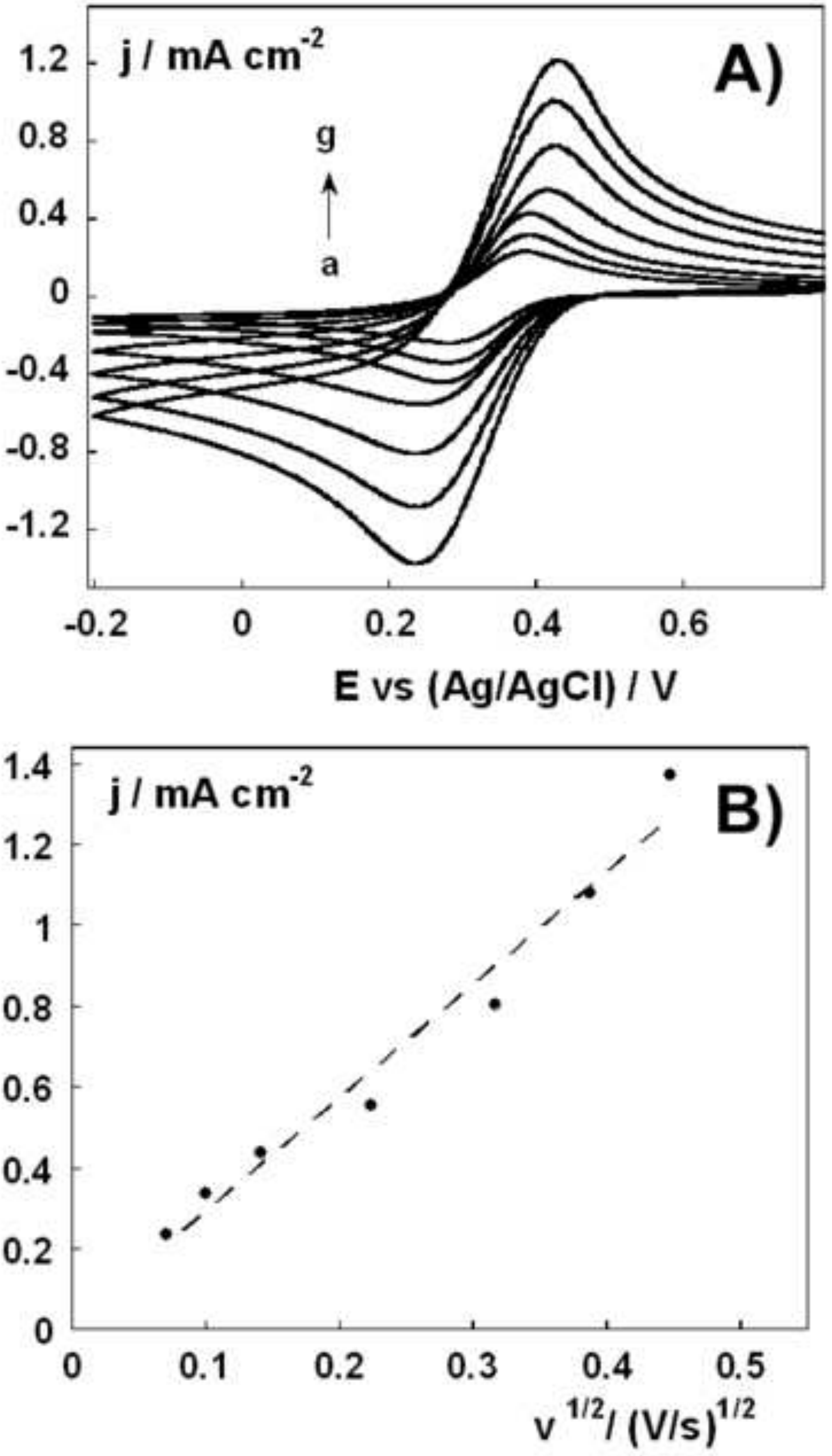
A)
j / mA cm^{-2}
1.2
0.8
0.4
0
-0.4
-0.8
-1.2
g
a
-0.2
0
0.2
0.4
0.6
E vs (Ag/AgCl) / V
B)
j / mA cm^{-2}
1.4
1.2
1
0.8
0.6
0.4
0.2
0
0
0.1
0.2
0.3
0.4
0.5
v $^{1/2}$/ (V/s)$^{1/2}$

Figure 5

Figure6

Click here to download high resolution image

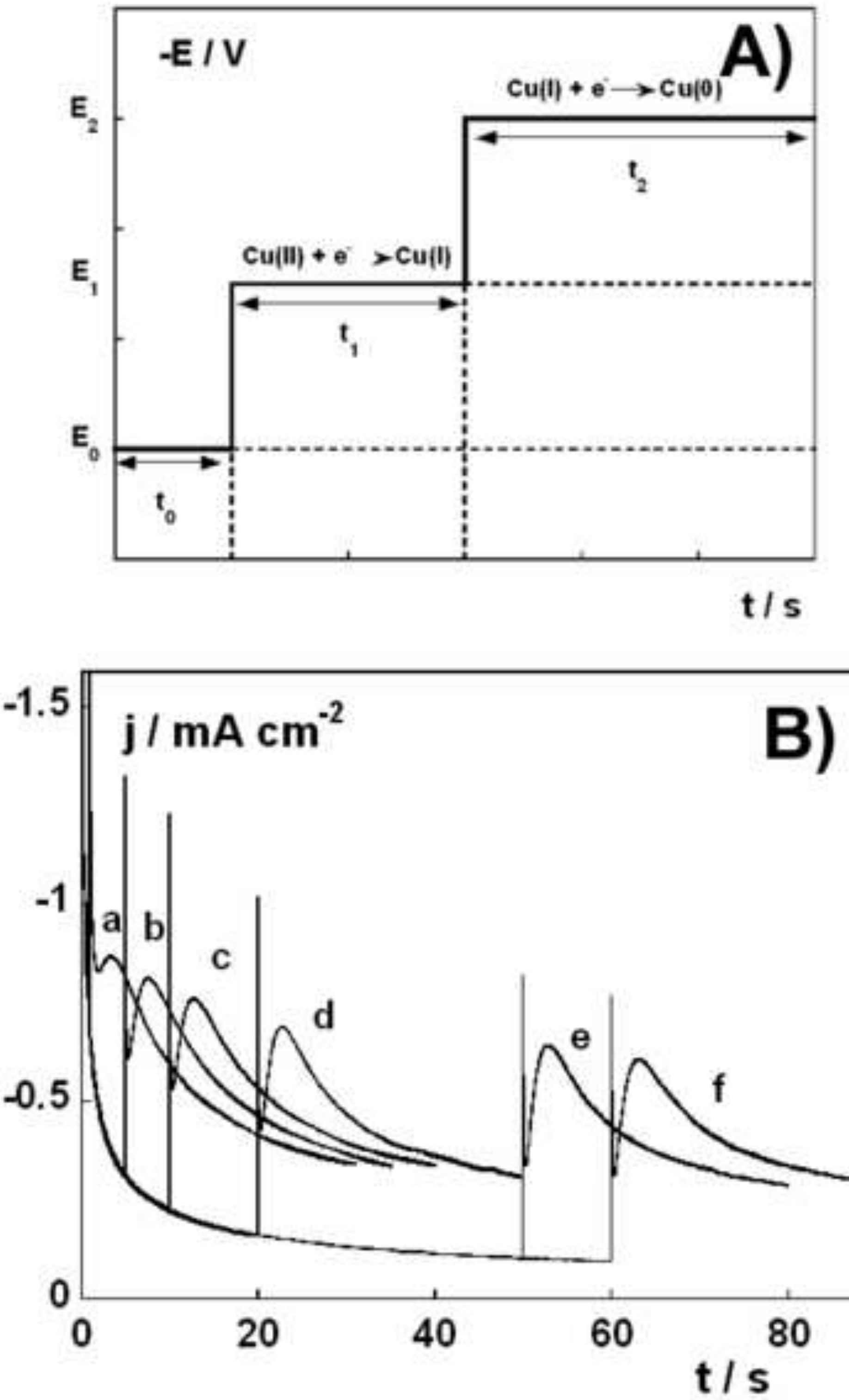

Figure 6

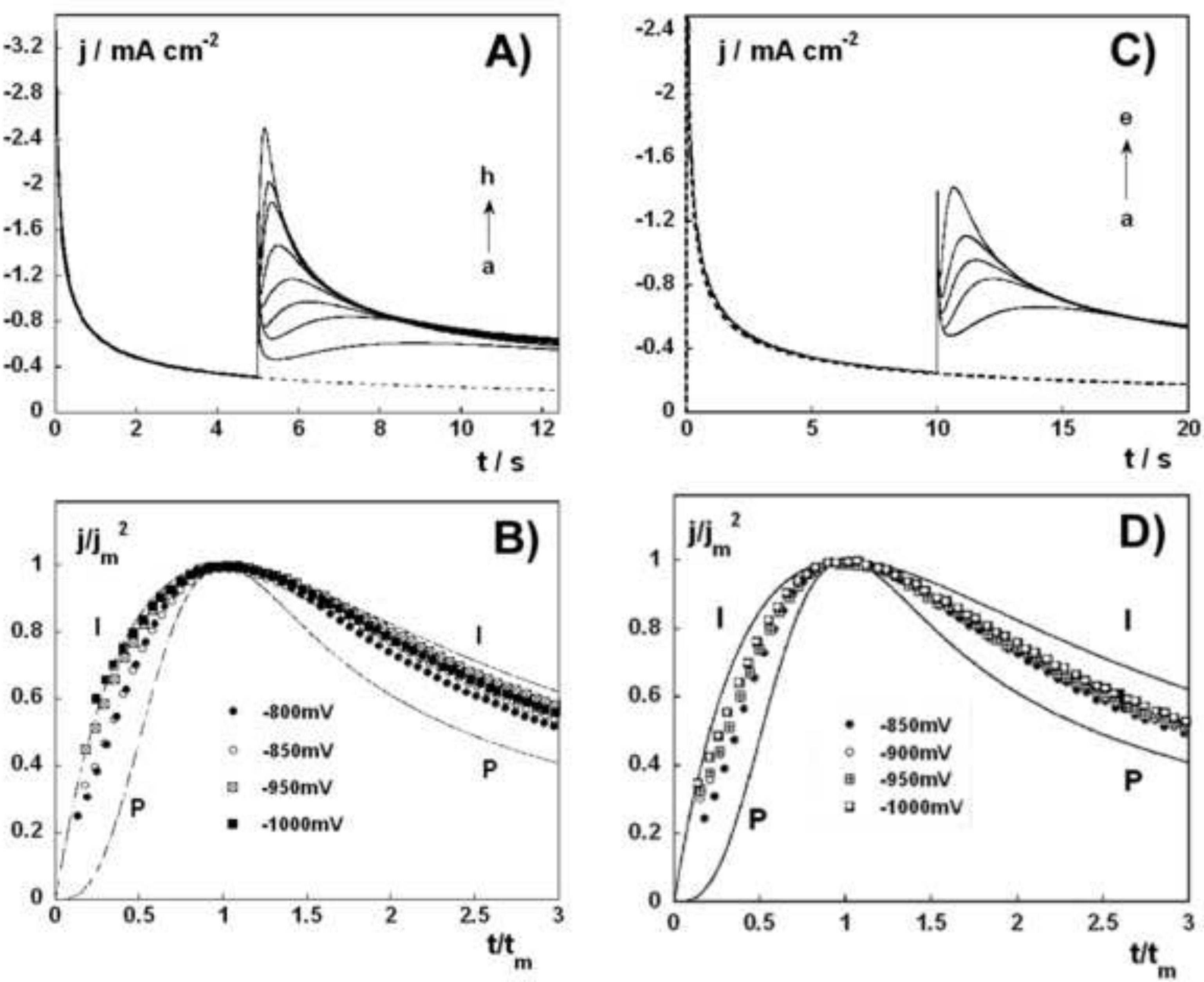
A)
j / mA cm^{-2}
-3.2
-2.8
-2.4
-2
-1.6
-1.2
-0.8
-0.4
0
0
2
4
6
8
10
12
t / s
h
a
C)
j / mA cm^{-2}
-2.4
-2
-1.6
-1.2
-0.8
-0.4
0
0
5
10
15
20
t / s
e
a
B)
j/j$_m^2$
1
0.8
0.6
0.4
0.2
0
0
0.5
1
1.5
2
2.5
3
t/t$_m$
I
I
P
P
● -800mV
○ -850mV
▨ -950mV
■ -1000mV
D)
j/j$_m^2$
1
0.8
0.6
0.4
0.2
0
0
0.5
1
1.5
2
2.5
3
t/t$_m$
I
I
P
P
● -850mV
○ -900mV
▨ -950mV
□ -1000mV

Figure 7

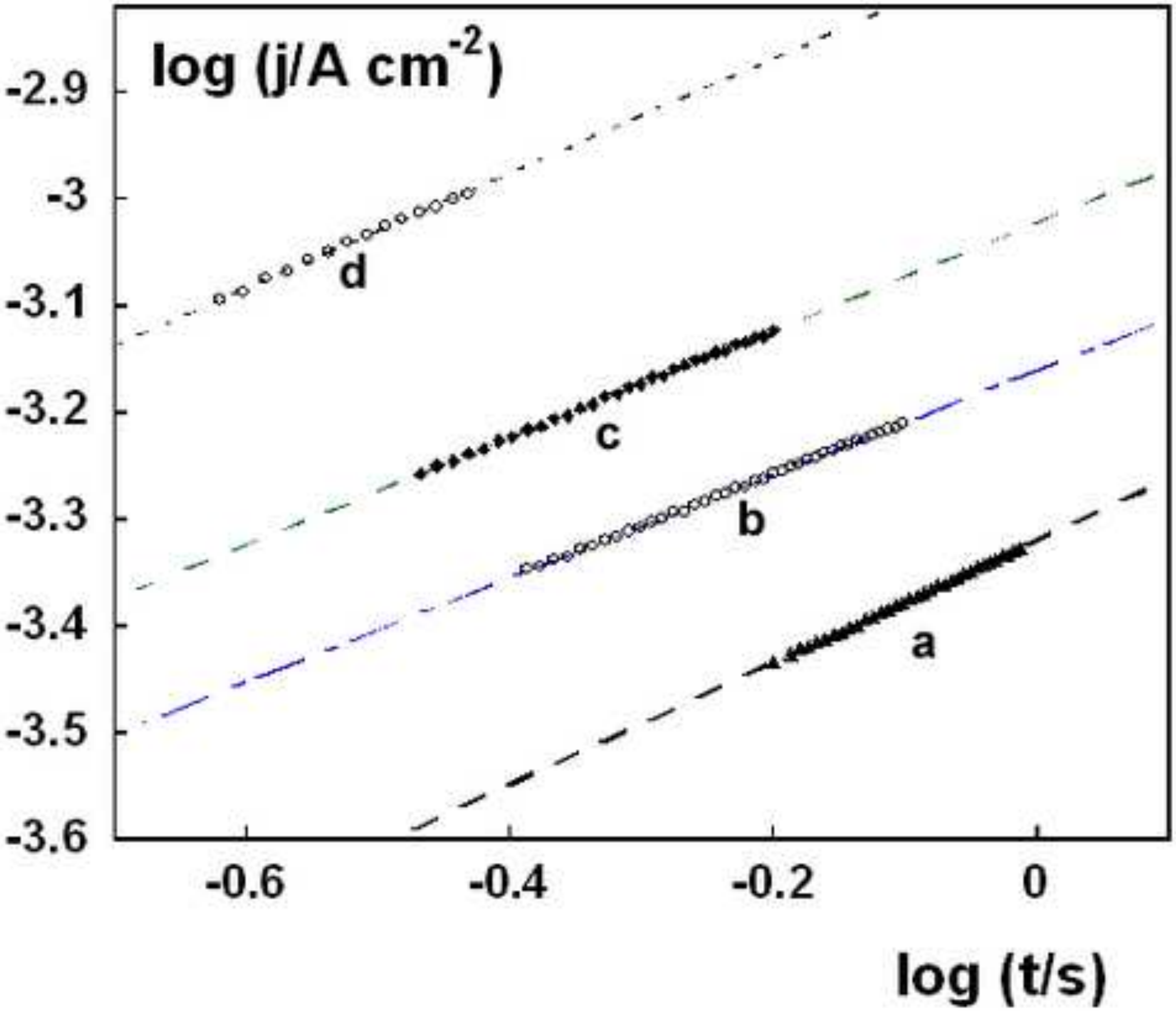

Figure 8

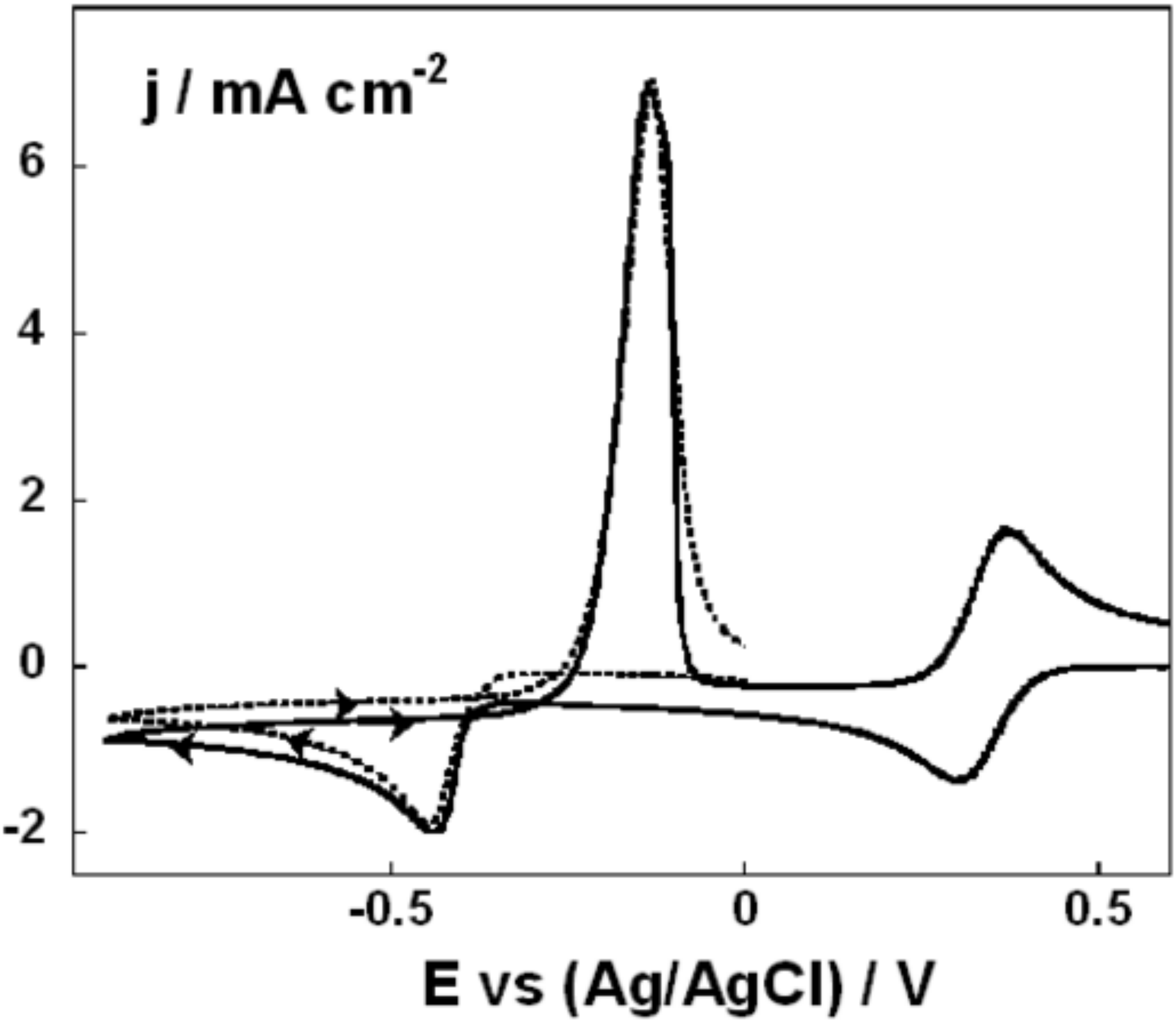

Figure 9

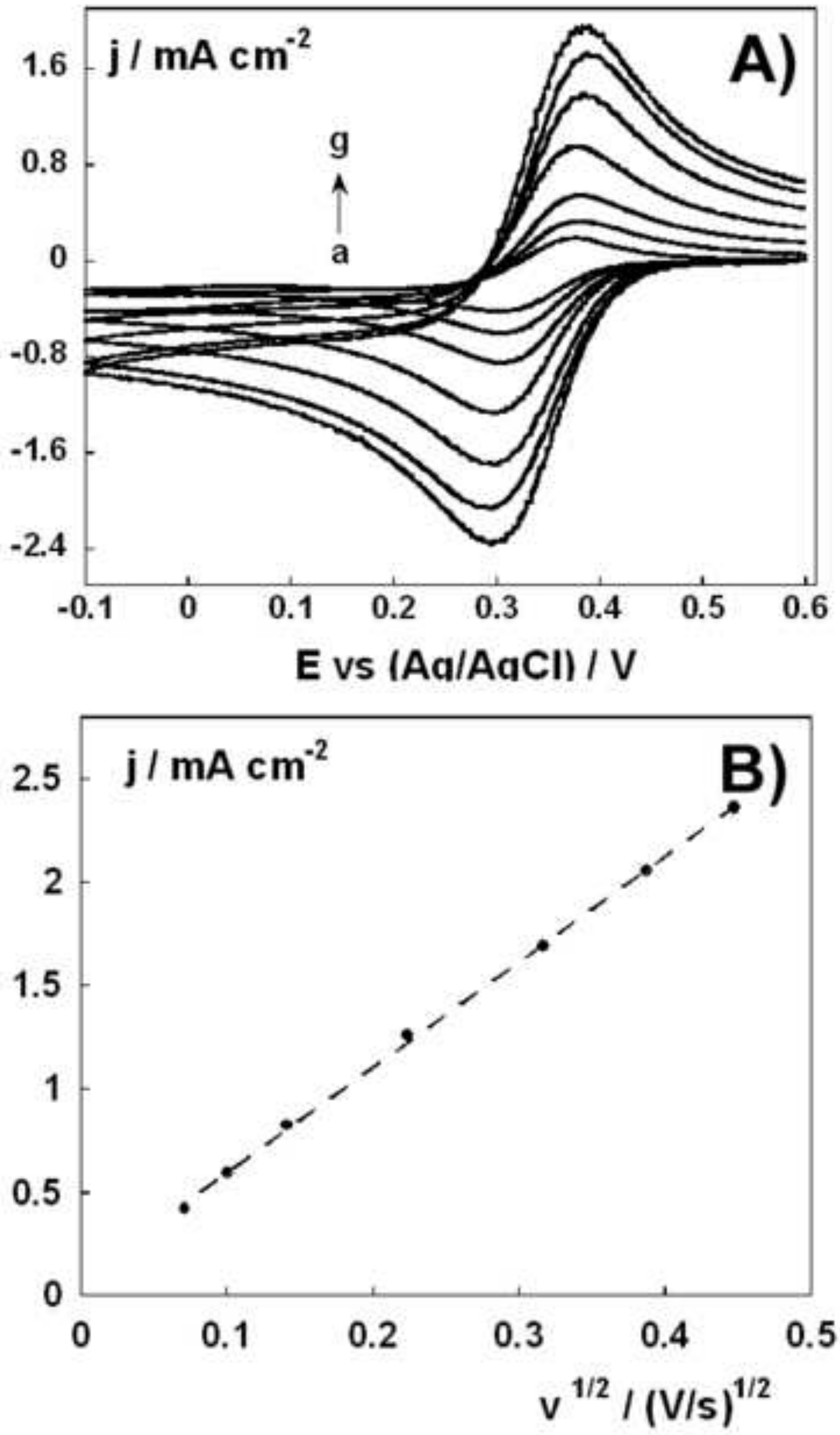
A)
j / mA cm^{-2}
1.6
0.8
0
-0.8
-1.6
-2.4
g
a
-0.1
0
0.1
0.2
0.3
0.4
0.5
0.6
E vs (Ag/AgCl) / V
B)
j / mA cm^{-2}
2.5
2
1.5
1
0.5
0
0
0.1
0.2
0.3
0.4
0.5
v $^{1/2}$ / (V/s)$^{1/2}$

Figure 10

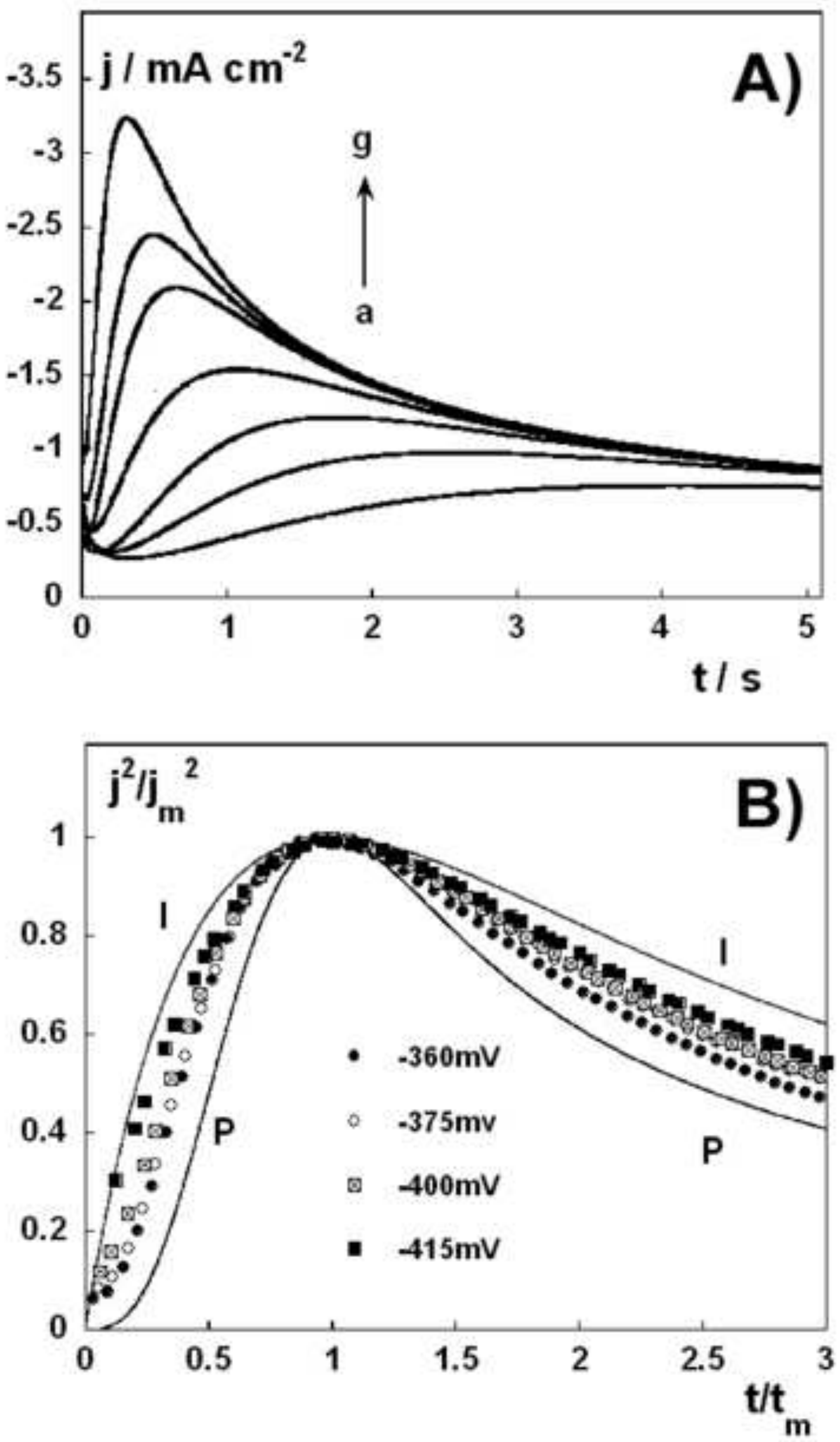
A)
j / mA cm^{-2}
-3.5
-3
-2.5
-2
-1.5
-1
-0.5
0
g
a
0
1
2
3
4
5
t / s
B)
$j^2/j_m^{\ 2}$
1
0.8
0.6
0.4
0.2
0
I
P
I
P
● -360mV
○ -375mv
▨ -400mV
■ -415mV
0
0.5
1
1.5
2
2.5
3
t/t_m

Figure 11

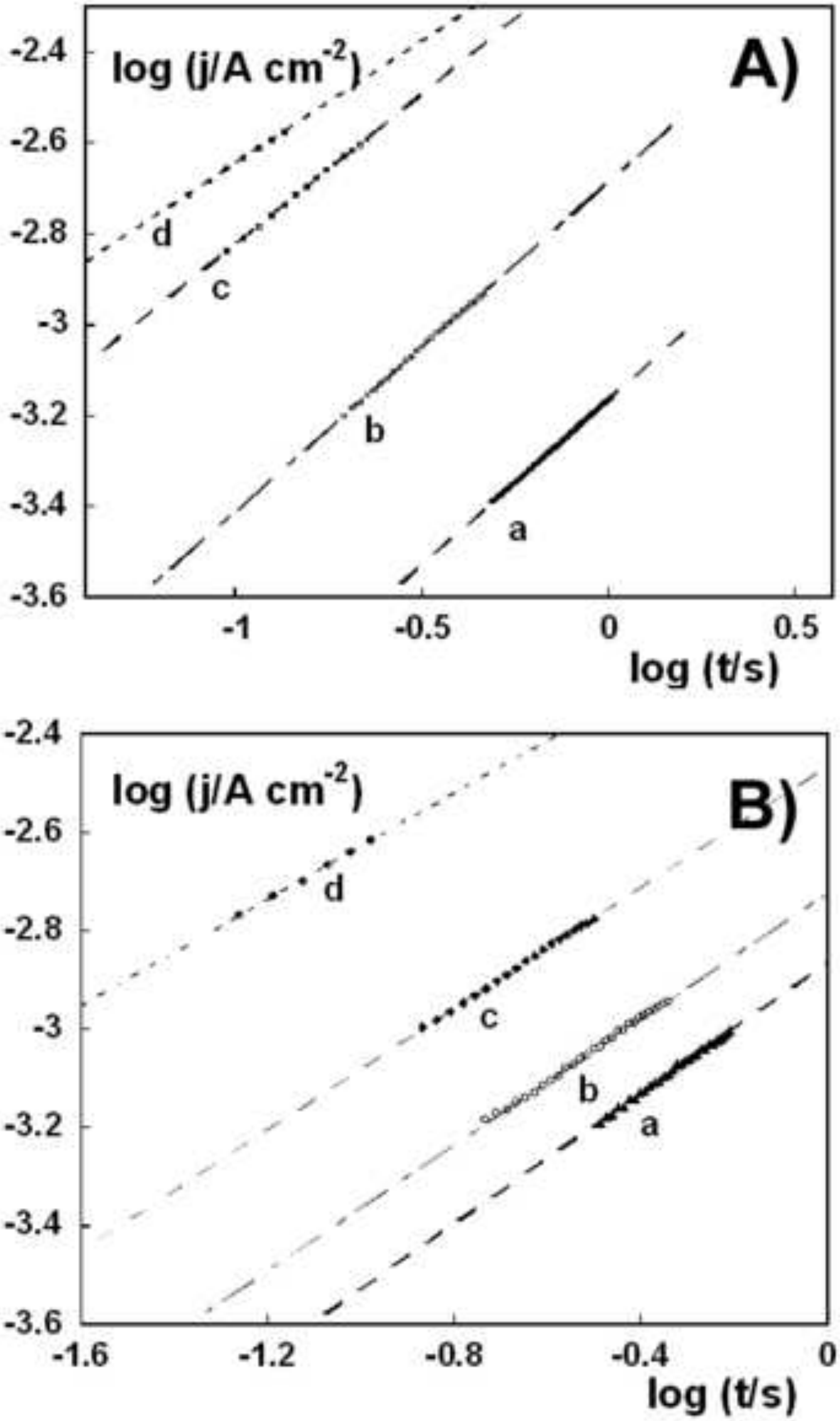
log (j/A cm^{-2})
A)
-2.4
-2.6
-2.8
-3
-3.2
-3.4
-3.6
-1
-0.5
0
0.5
log (t/s)
d
c
b
a
log (j/A cm^{-2})
B)
-2.4
-2.6
-2.8
-3
-3.2
-3.4
-3.6
-1.6
-1.2
-0.8
-0.4
0
log (t/s)
d
c
b
a

Figure 12

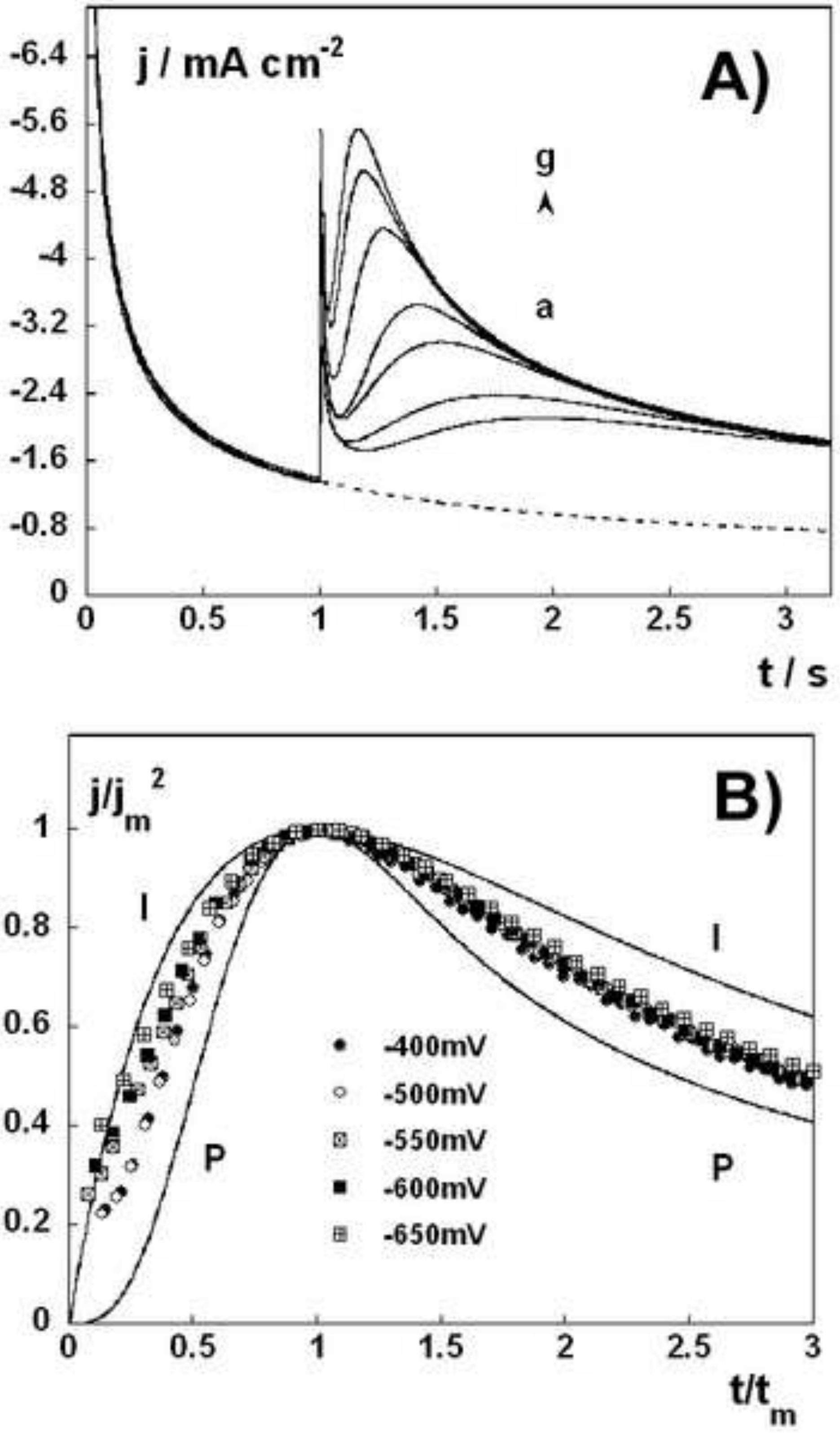
j / mA cm^{-2}
A)
-6.4
-5.6
-4.8
-4
-3.2
-2.4
-1.6
-0.8
0
g
a
0
0.5
1
1.5
2
2.5
3
t / s
B)
j/j$_m^2$
1
0.8
0.6
0.4
0.2
0
I
P
I
P
● -400mV
○ -500mV
⊠ -550mV
■ -600mV
⊞ -650mV
0
0.5
1
1.5
2
2.5
3
t/t$_m$

Figure 13

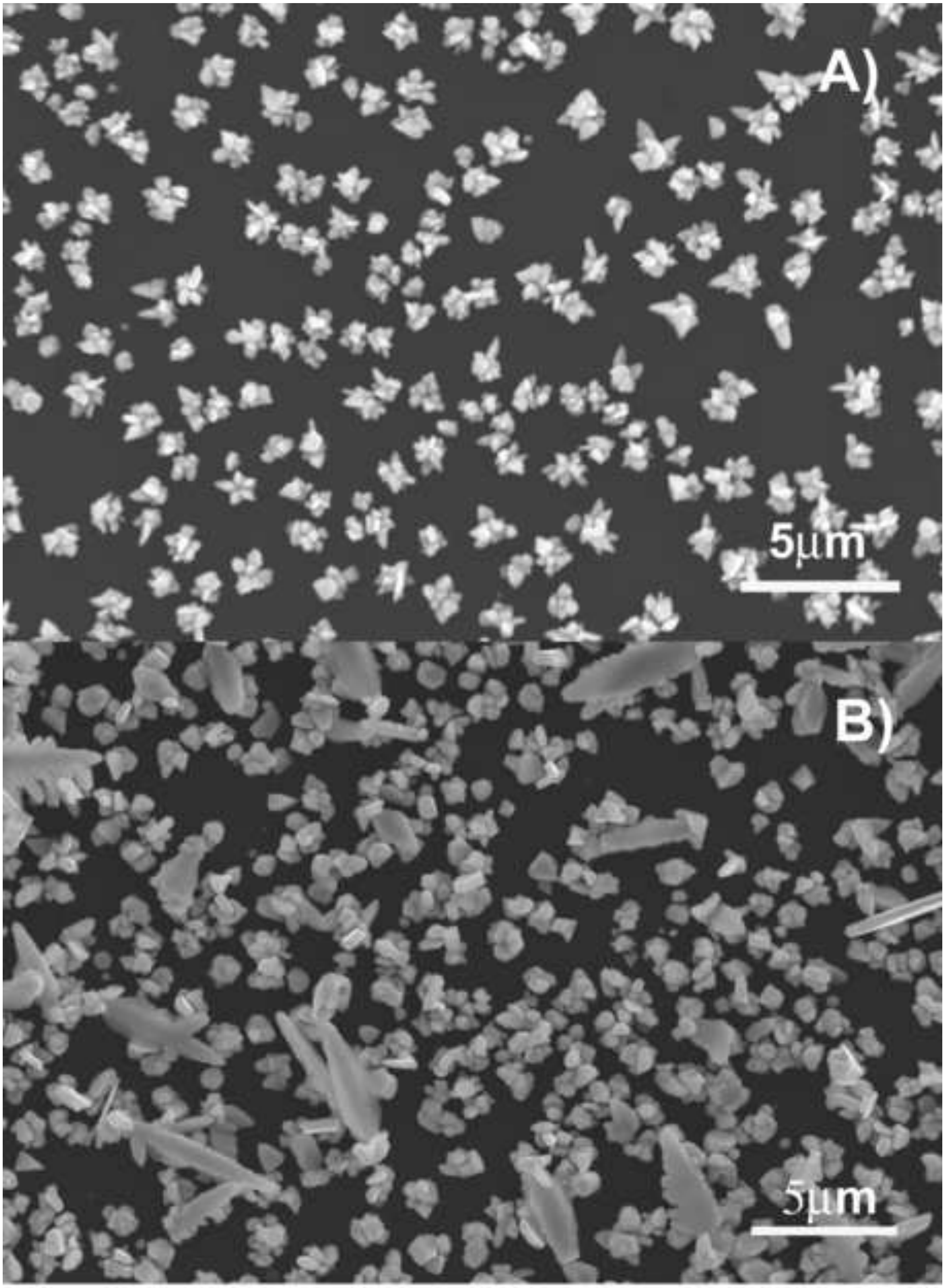

Figure 14AB

Figure14C

Click here to download high resolution image

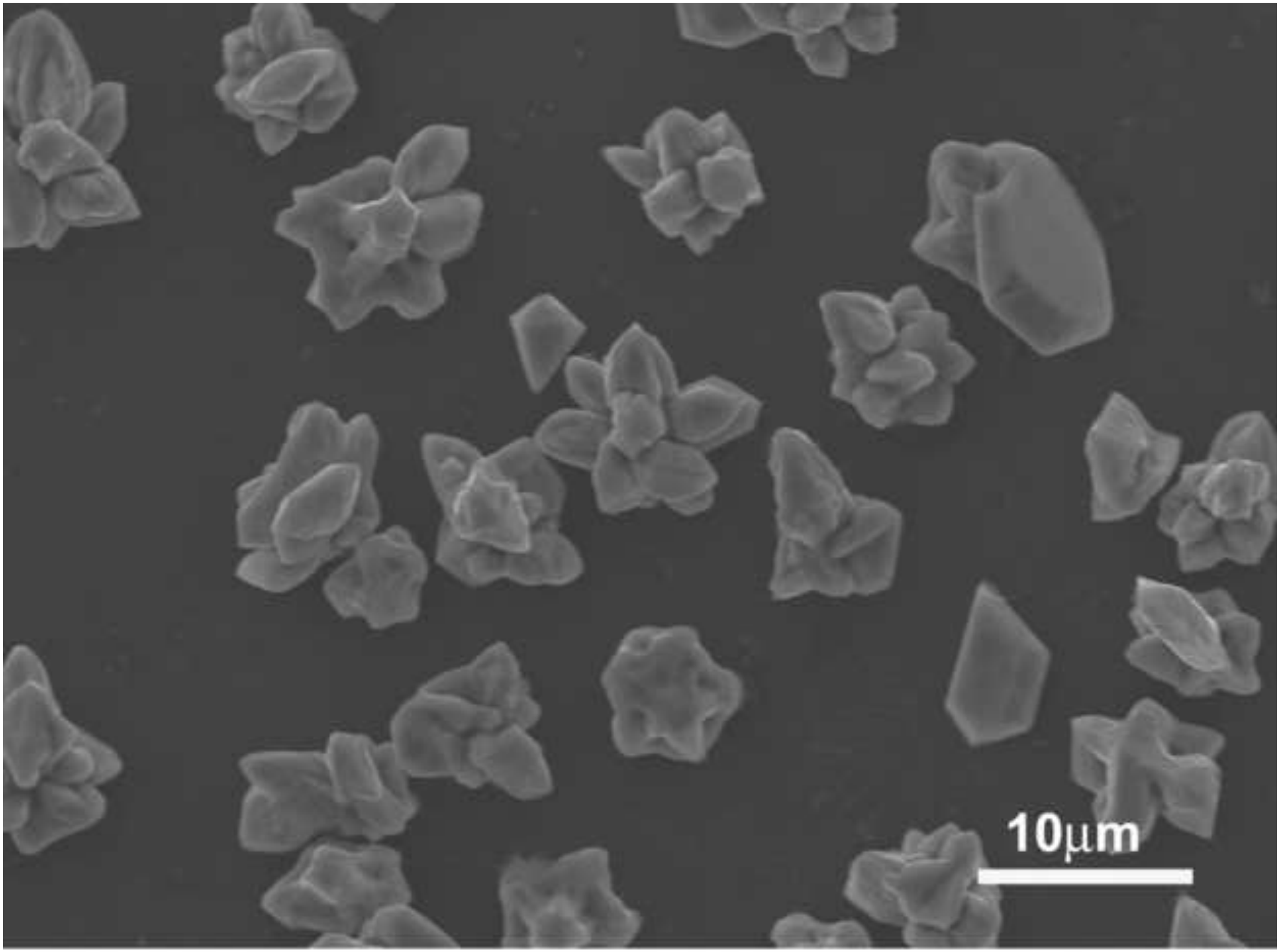

Figure 14C

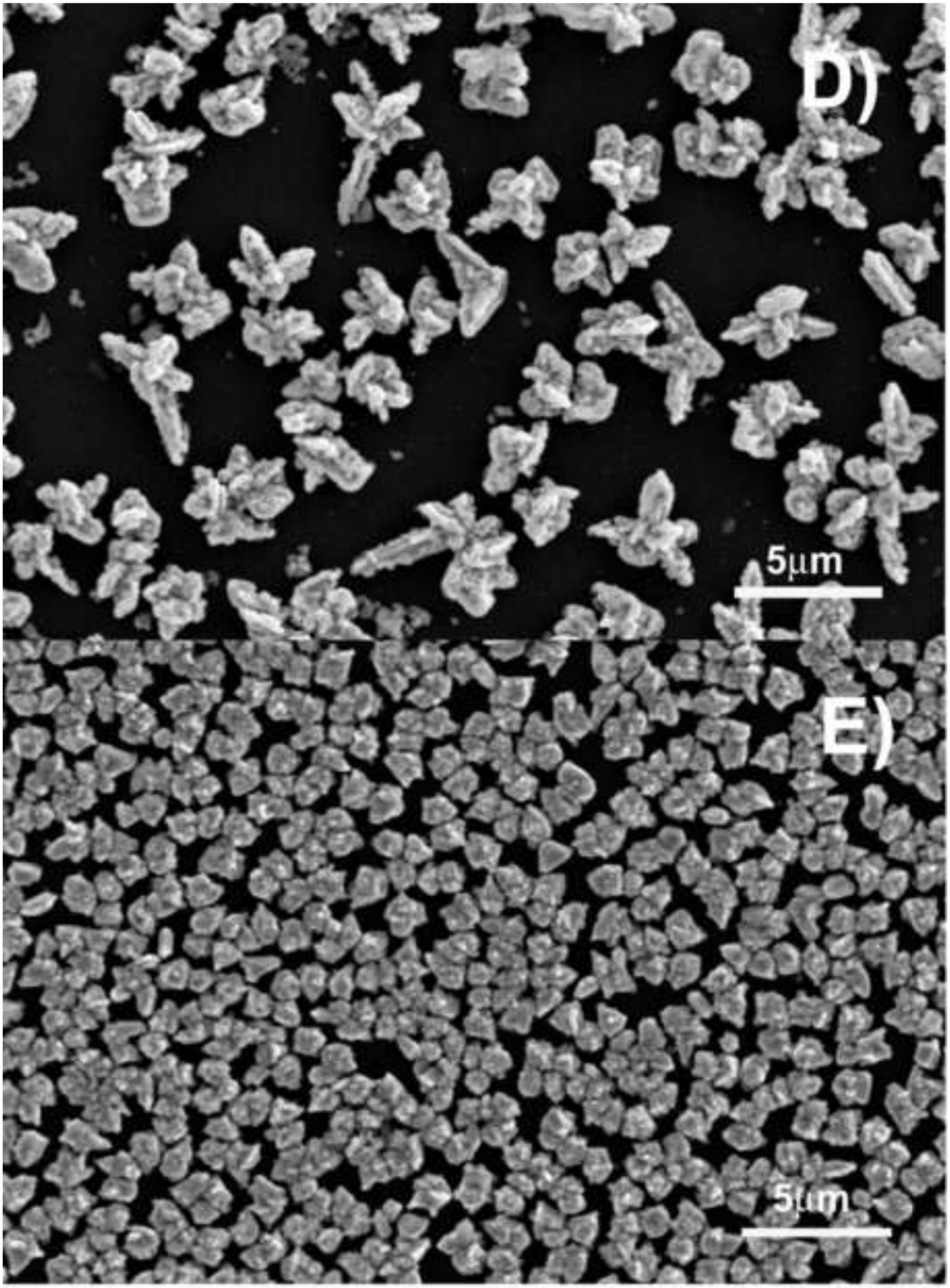

Figures 14DE